# Polar discs and circumbinary formation in highly misaligned discs

**Jeremy L. Smallwood**
*Dodge Family Prize Fellowship in Astrophysics*
*University of Oklahoma*

**The formation and long-term evolution of circumbinary planetary systems across the H-R diagram**
**Jan. 14th 2025**

# Outline

- Observational motivation
- CBD alignment process
- Accretion from misaligned CBDs
- Dust dynamics in misaligned CBDs
- Implications for circumbinary planet formation


Credit: ALMA / ESO / NAOJ / NRAO / I. Czekala & G. Kennedy / AUI / NSF / S. Dagnello.)

# Circumbinary Planets

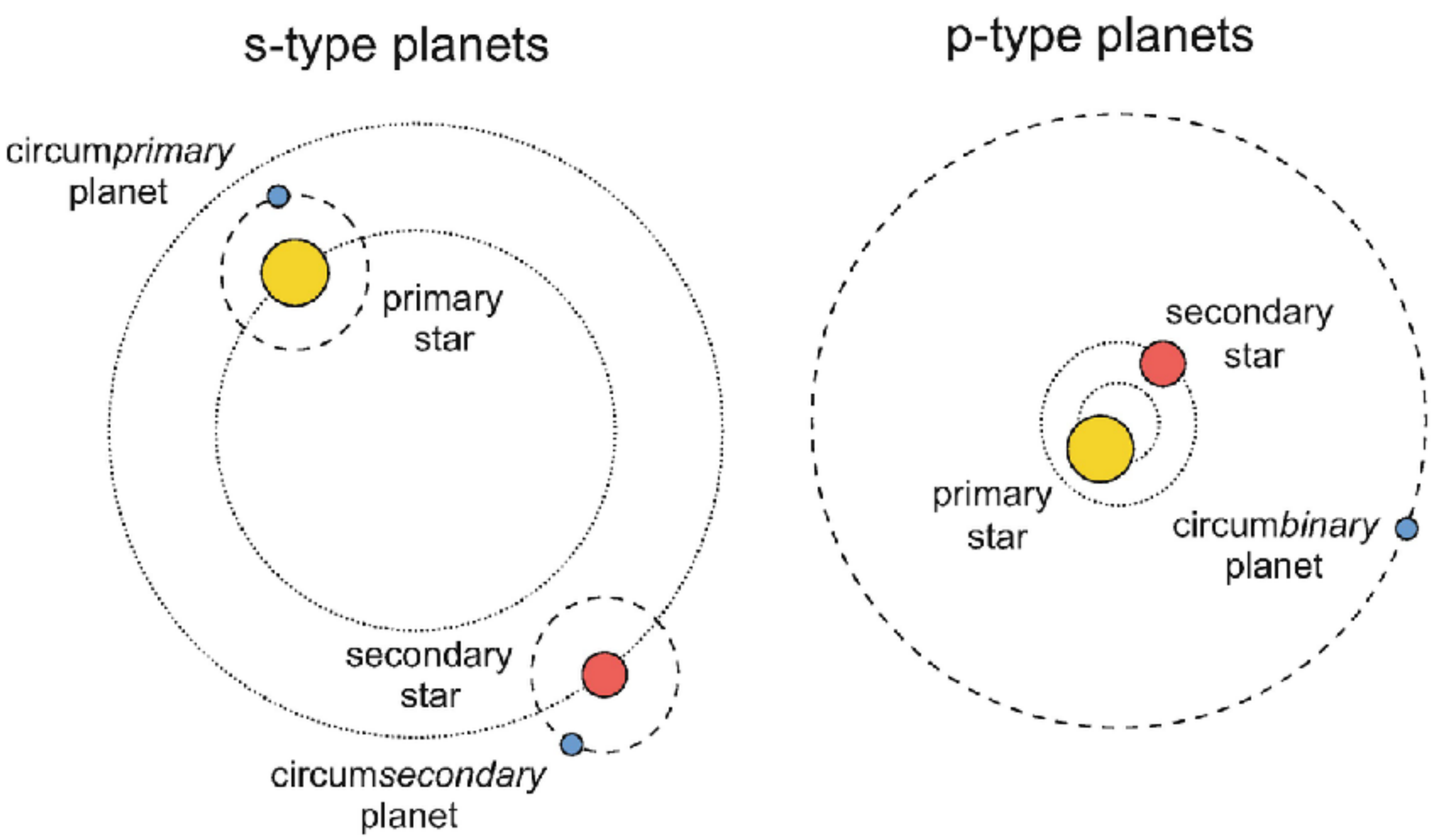


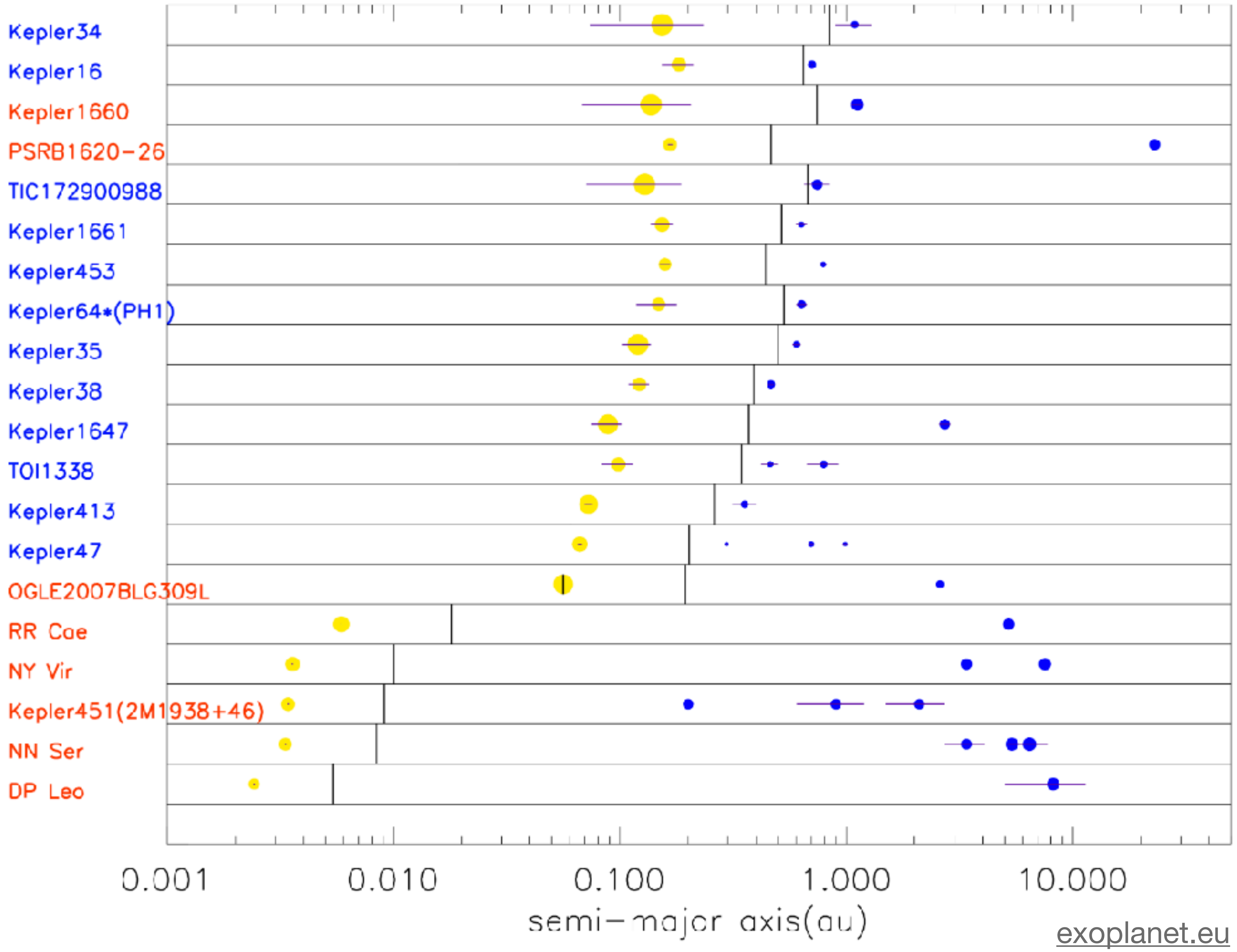


exoplanet.eu

# Circumbinary Disk Misalignment

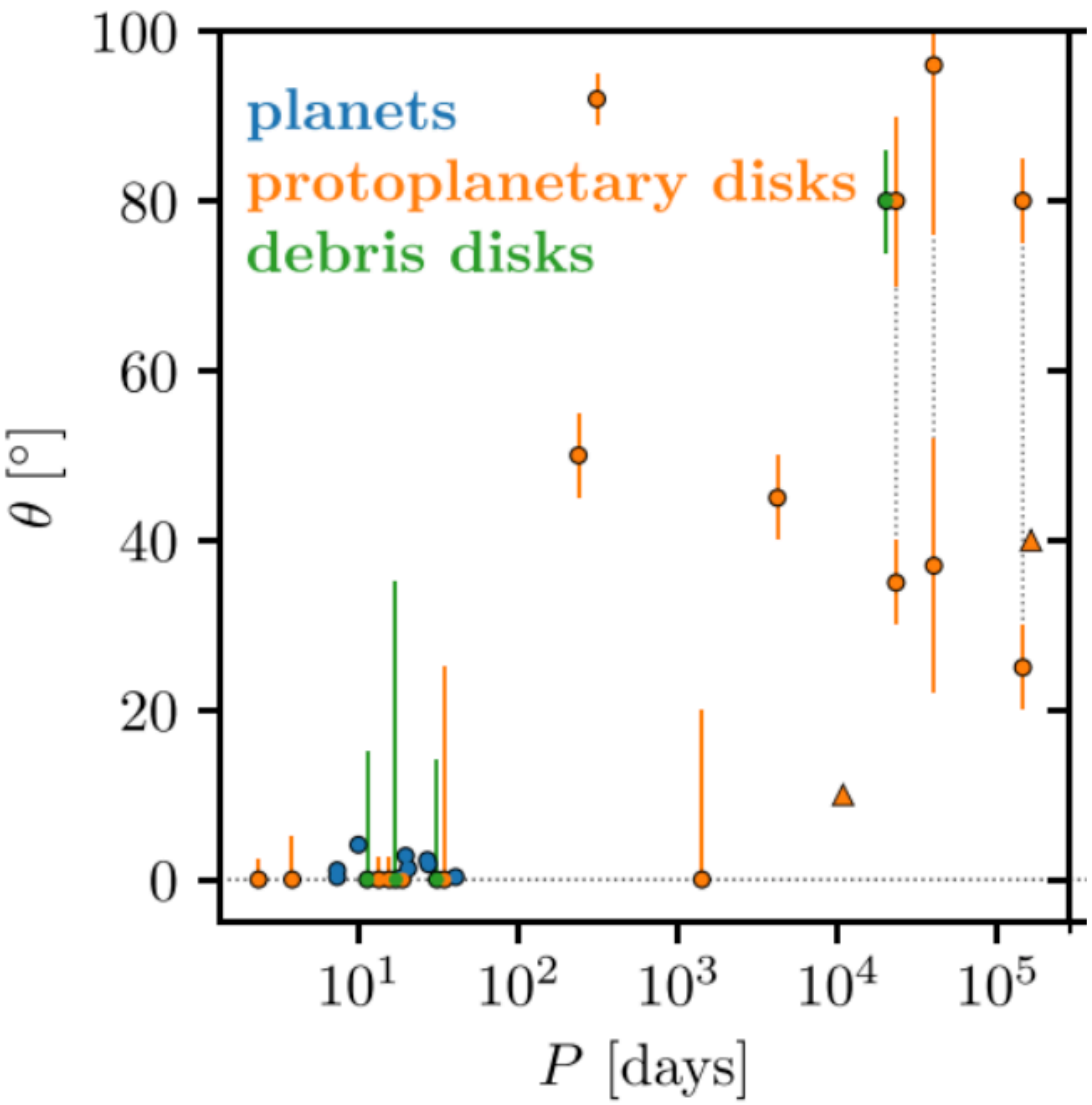


Czekala et al. 2019

- All observed circumbinary planets are aligned to the binary, however, misaligned disks are common.
- Why is there a discrepancy?
- A new population of planets — misaligned/polar planets around binary star systems.

# HD 98800

- Quadruple star system
- 47 pc and comprises two binaries:
    - HD 98800 AaAb
    - HD 98800 BaBb
- $a_{AB}$ = 54 au, $P_{AB}$ = 246 yrs, $e_{AB}$ = 0.52
- The orbit of the BaBb binary is well constrained.
    - a = 1 au
    - e = 0.785
    - $M_{Ba}$ = 0.699 M
    - $M_{Bb}$ = 0.582 M

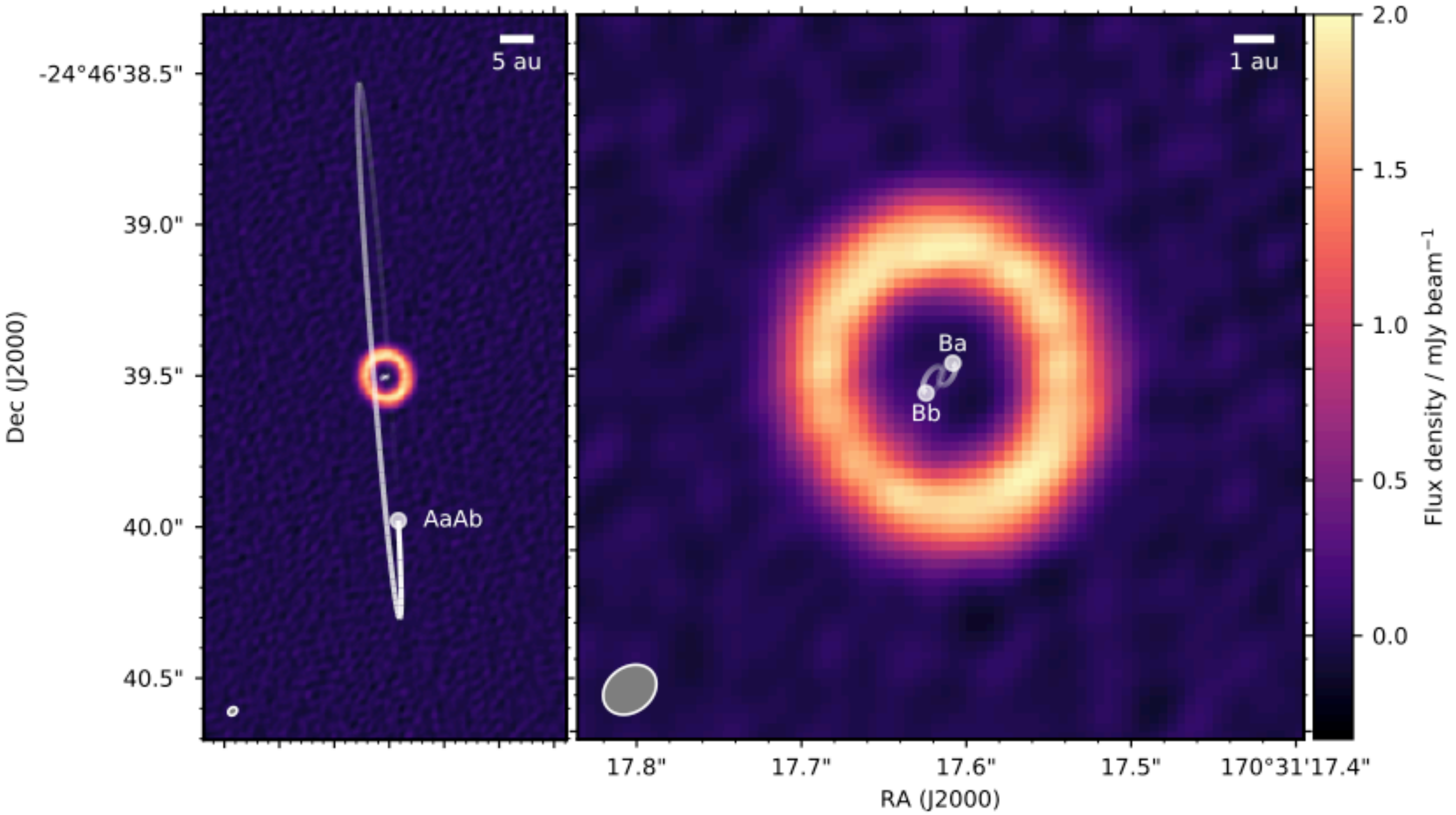


**ALMA 1.3 millimetre continuum image of the HD 98800 BaBb dust disc, showing a narrow dust ring.**

Kennedy et al. (2019)

- Tilt inferred to be either 48 deg or 90 deg.
- Very compact dust ring at 2 au, extending to 3.5 au
- Gas disc: 1.6 to 6.4 au

# HD 98800 BaBb Circumbinay Disc

- Torques on the inner parts of polar disc are much weaker than in the coplanar case.

—> Smaller cavity size for a polar disc.

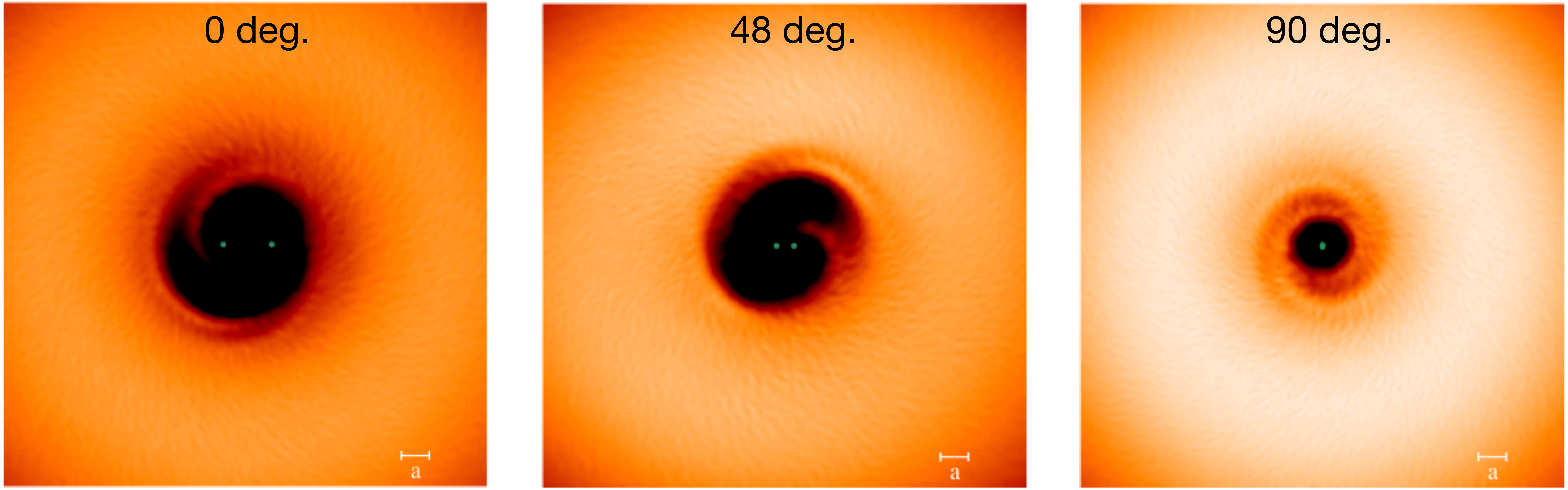


Franchini, Lubow and Martin (2019)

# 99 Herculis

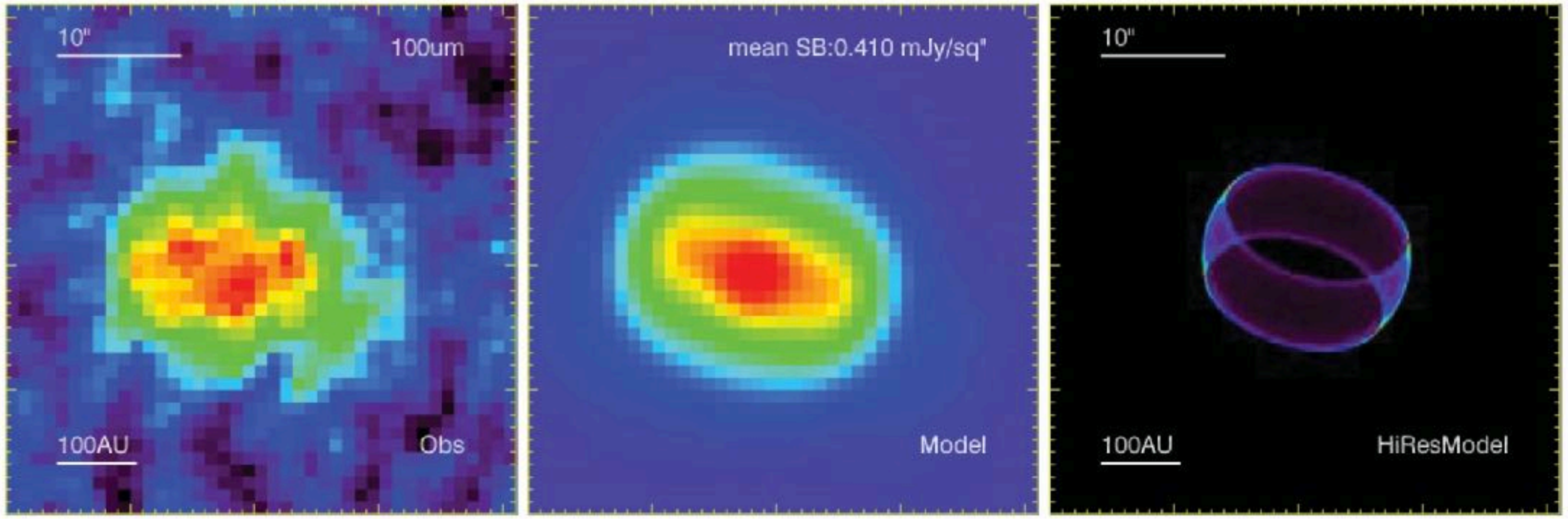


- 99 Her consists of an F7V primary star and a K4V secondary star, with an estimated age of 6-10 (Takeda 2007)
- a = 16.5 au
- e = 0.766
- $P_{orb}$= 56.3 yr

- Kennedy et al. (2012) estimated the debris disc structure, inclination, and PA using two-dimensional Gaussian models
- The debris disc is tilted 87° with respect to the binary pericentre direction (Kennedy et al. 2012). The observed disc tilt is only 3° away from polar alignment.

decreasing particle tilt

i = 90 deg.

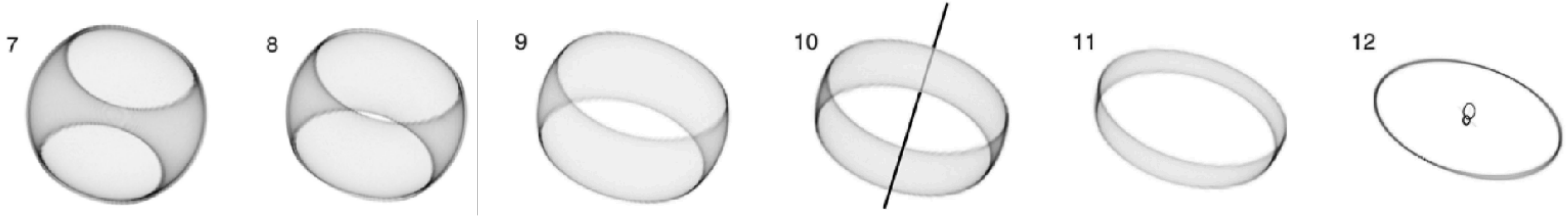

# Misaligned CBD systems

KH 15D

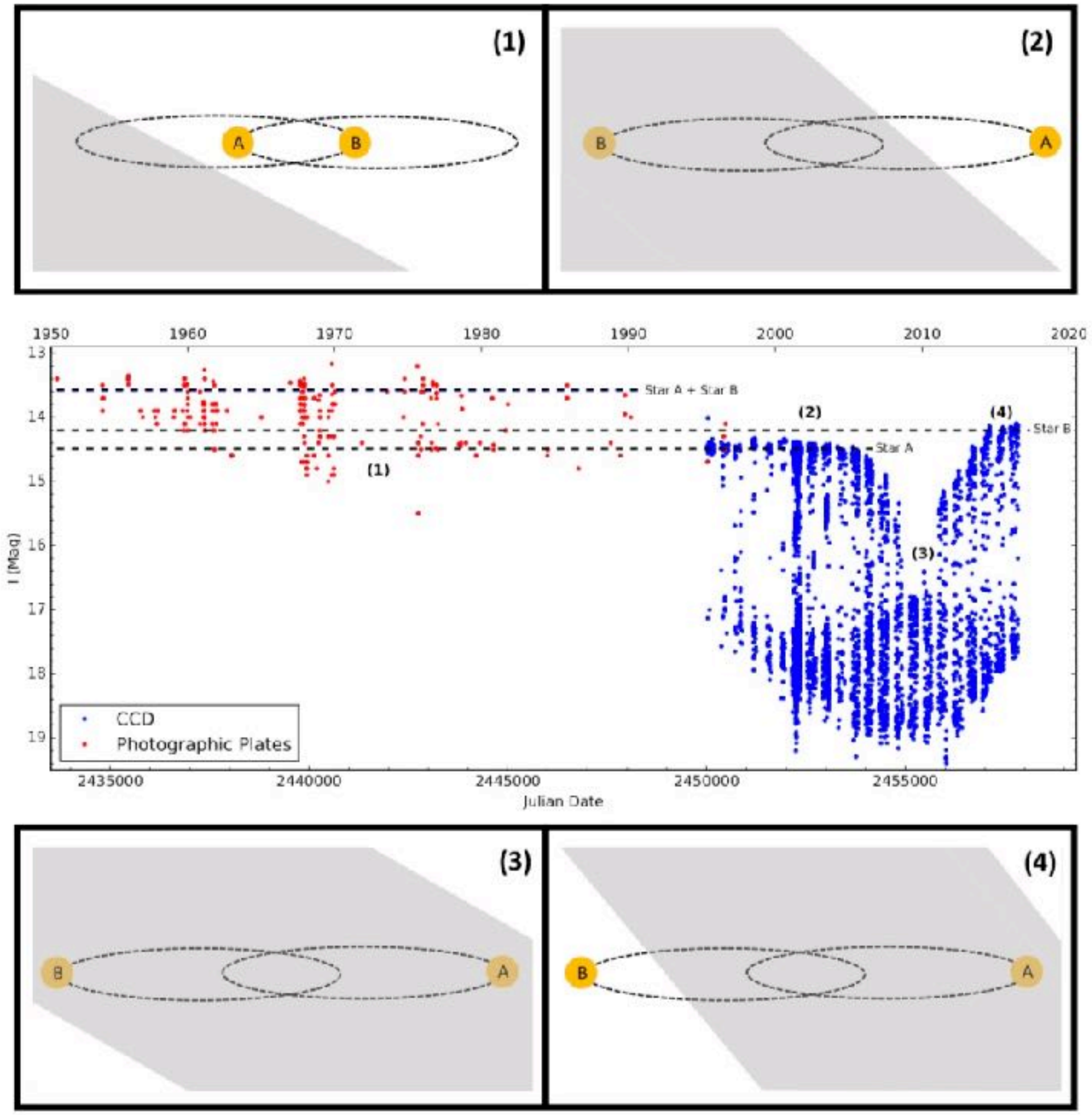


Chiang & Murray-Clay (2004); Aronow et al. (2018);
Smallwood et al. (2019b) ; Poon et al. (2020)

IRS 43

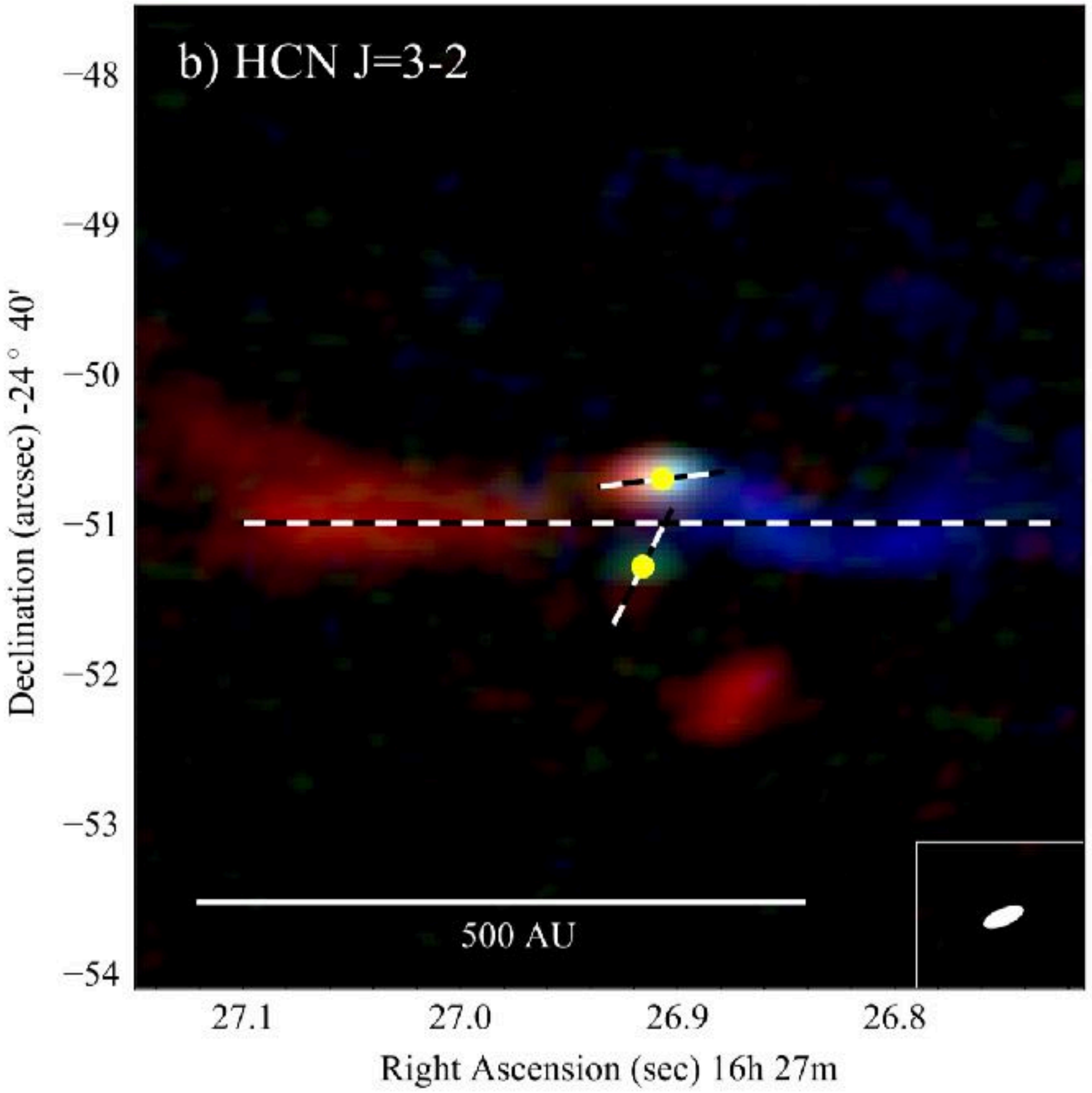


Brinch et al. (2016)

# Circumbinary Disc Alignment

- A misaligned circumbinary disc will undergo alignment either **coplanar** (Lubow & Ogilvie 2000; Foucart & Lai 2014) or **polar** (Aly et al. 2015; Martin & Lubow 2017; Zanazzi & Lai 2018) to the binary orbital plane.

$$i_{\min} = \arccos\left[\frac{\sqrt{5}e_{b0}\sqrt{4e_{b0}^2 - 4j_0^2(1-e_{b0}^2)+1} - 2j_0(1-e_{b0}^2)}{1+4e_{b0}^2}\right]$$

**disc AM:** $$J_{d0} = \int_{r_{in}}^{r_{out}} 2\pi r^3 \Sigma_0(r)\Omega dr,$$

**binary AM:** $$J_{b0} = \mu\sqrt{G(M_1+M_2)a_{b0}(1-e_{b0}^2)}$$

Martin & Lubow 2019

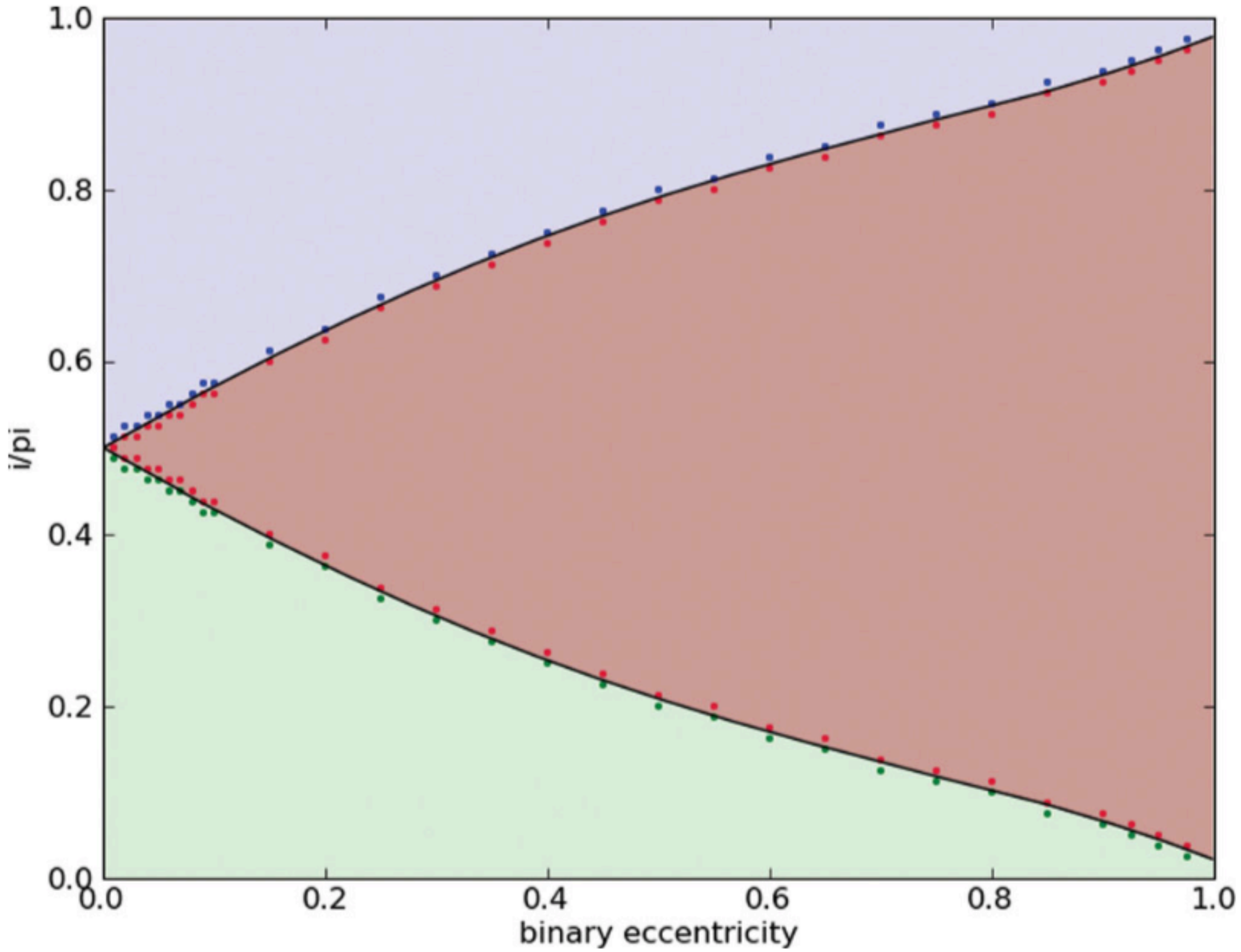


Doolin & Blundell 2011

# Circumbinary Disc Alignment


Smallwood et al. (2024e)

- Circumbinary discs will align to three stable orientations.
- On average, the polar alignment timescale is shorter than the coplanar alignment timescale.

# Alignment Timescales

disc aspect ratio

binary angular frequency

$$\tau = \frac{1}{\alpha}\left(\frac{H}{R}\right)^2 \frac{\Omega_\mathrm{b}}{\Omega_\mathrm{p}^2}$$

viscosity

global disc precession frequency

$$\Omega_\mathrm{b} = \sqrt{G(M_1 + M_2)/a^3}$$

$$\Omega_\mathrm{p} = \frac{3\sqrt{5}}{4} e_\mathrm{b}\sqrt{1 + 4e_\mathrm{b}^2}\,\frac{M_1 M_2}{M^2}\left\langle\left(\frac{a_\mathrm{b}}{r}\right)^{7/2}\right\rangle\Omega_\mathrm{b} \quad \textbf{(Polar)}$$

$$\Omega_\mathrm{p} = \frac{3}{4}\sqrt{1 + 3e_\mathrm{b}^2 - 4e_\mathrm{b}^4}\,\frac{M_1 M_2}{M^2}\left\langle\left(\frac{a}{R}\right)^{7/2}\right\rangle\Omega_\mathrm{b} \quad \textbf{(Coplanar)}$$

$$\left\langle\left(\frac{a_\mathrm{b}}{r}\right)^{7/2}\right\rangle = \frac{\int_{r_\mathrm{in}}^{r_\mathrm{out}} \Sigma(r) r^3 \Omega(r) (a_\mathrm{b}/r)^{7/2}\, dr}{\int_{r_\mathrm{in}}^{r_\mathrm{out}} \Sigma(r) r^3 \Omega(r)\, dr}$$

$$\Omega = \sqrt{G(M_1 + M_2)/R^3}$$

Lubow & Martin (2019)

Smallwood et al. (2019b)

# Alignment Timescales

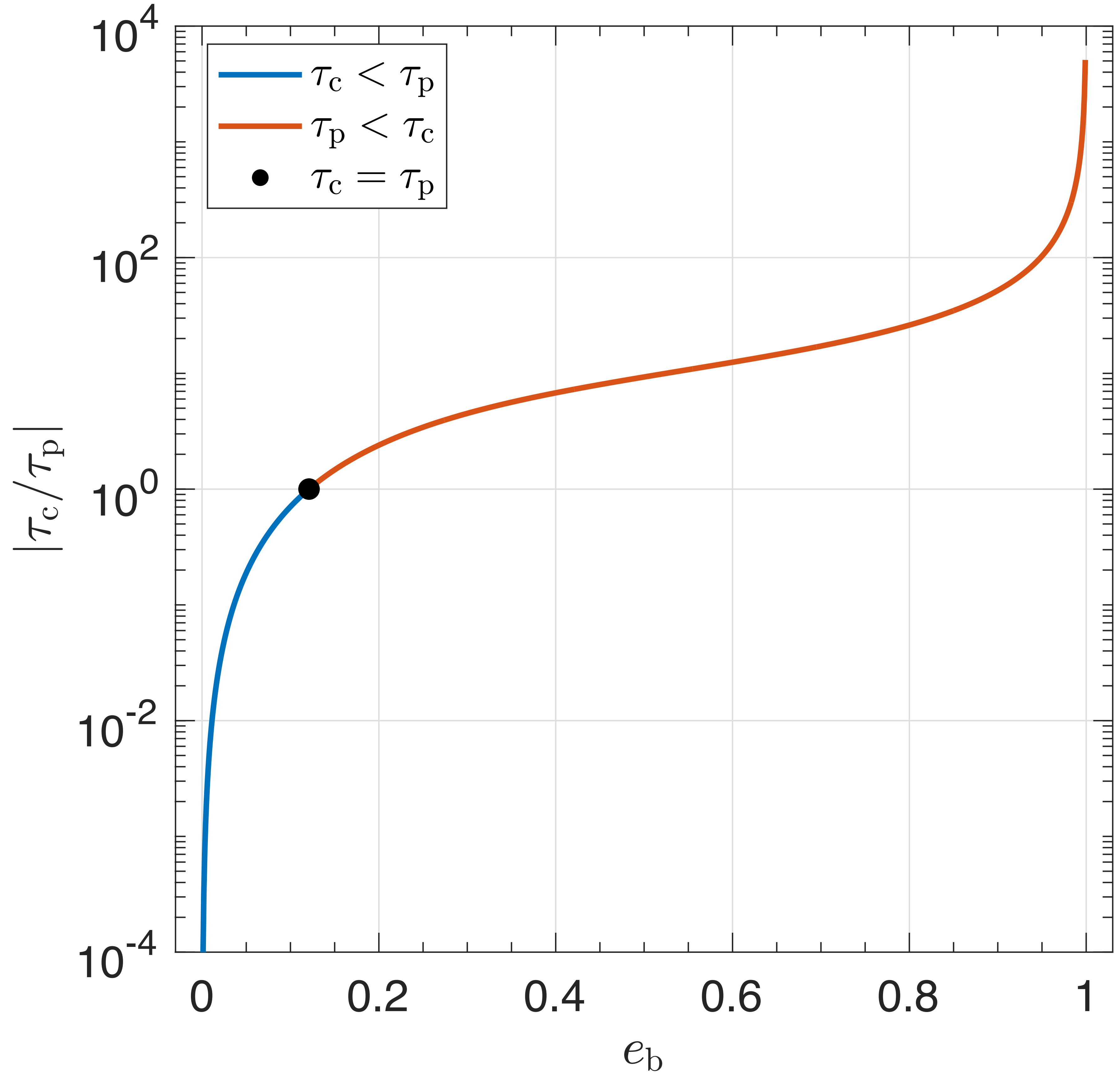


Smallwood et al. (2024e)

$$\frac{\tau_c}{\tau_p} = \frac{5e_b^2(1+4e_b^2)}{1+3e_b^2-4e_b^4}\left(\frac{10-r_c}{10-r_p}\right)^2\left(\frac{-625r_p^{5/2}+\sqrt{10}}{-625r_c^{5/2}+\sqrt{10}}\right)^2\left(\frac{r_c}{r_p}\right)^5.$$

# Coplanar Alignment


Smallwood et al. (2019)

# Coplanar Alignment

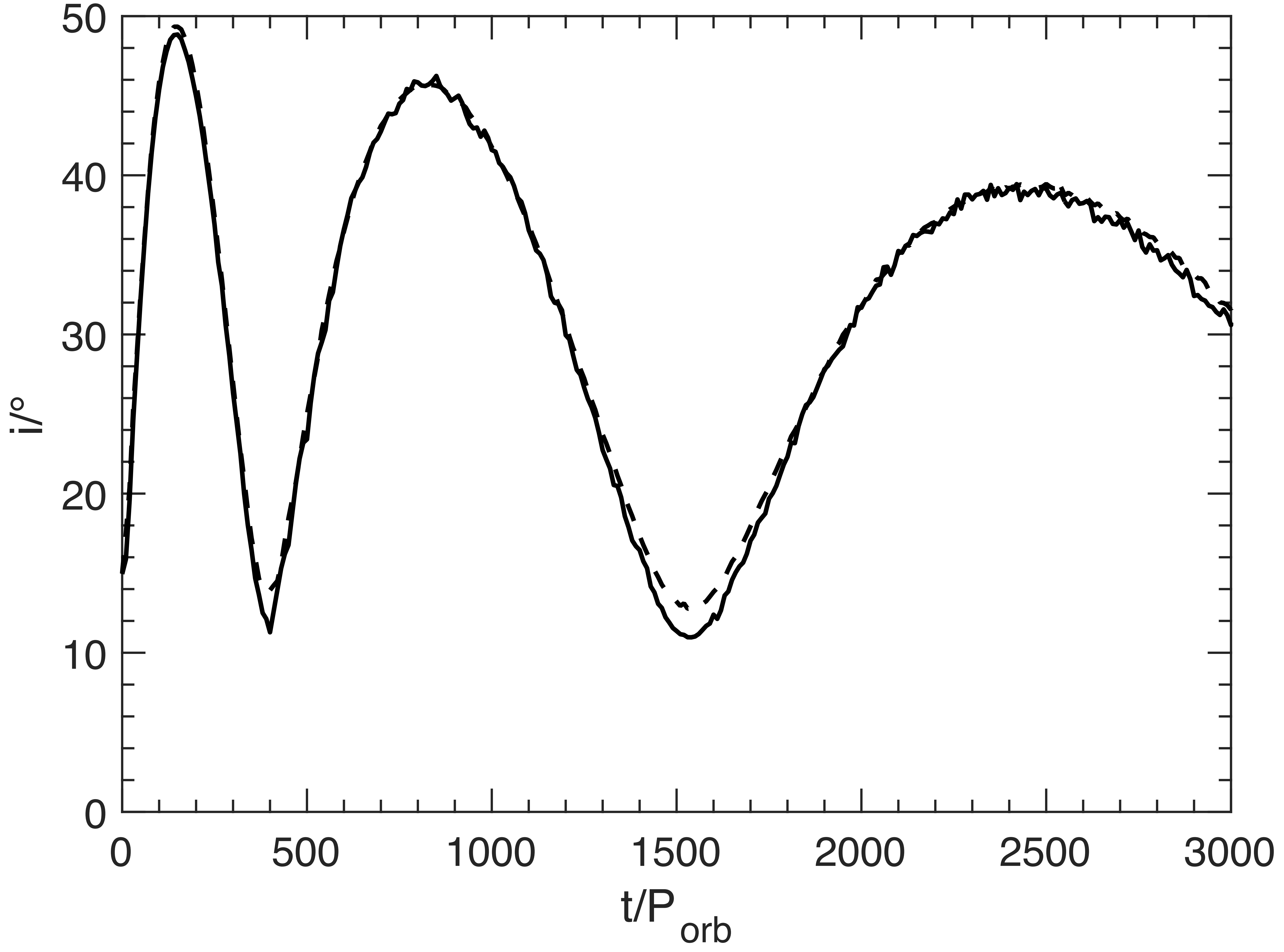


- If the timescale for disc alignment is **shorter** than the disc's age, planets may form **aligned** with the binary system.
- If the timescale for disc alignment is **longer** than the disc's age, planets are likely to form **misaligned** with the binary system.

Smallwood et al. (2019)

# Polar Alignment


Smallwood et al. (2020)

# Polar Alignment

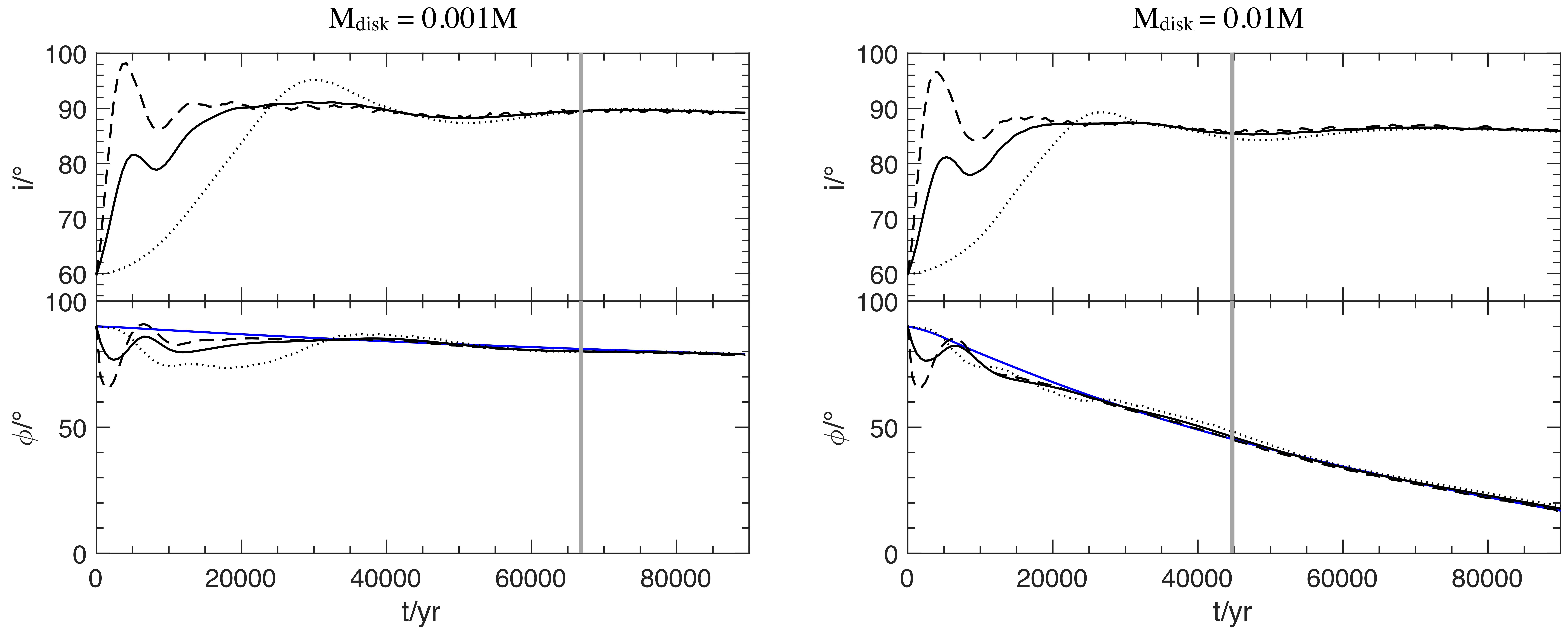


Smallwood et al. (2020)

**Smallwood et al. (2024e)**

- Accretion rate as a function of time.
- Coplanar-aligning discs undergo preferential alternating accretion.
- Polar-aligning discs may have transient periods of preferential alternating accretion.

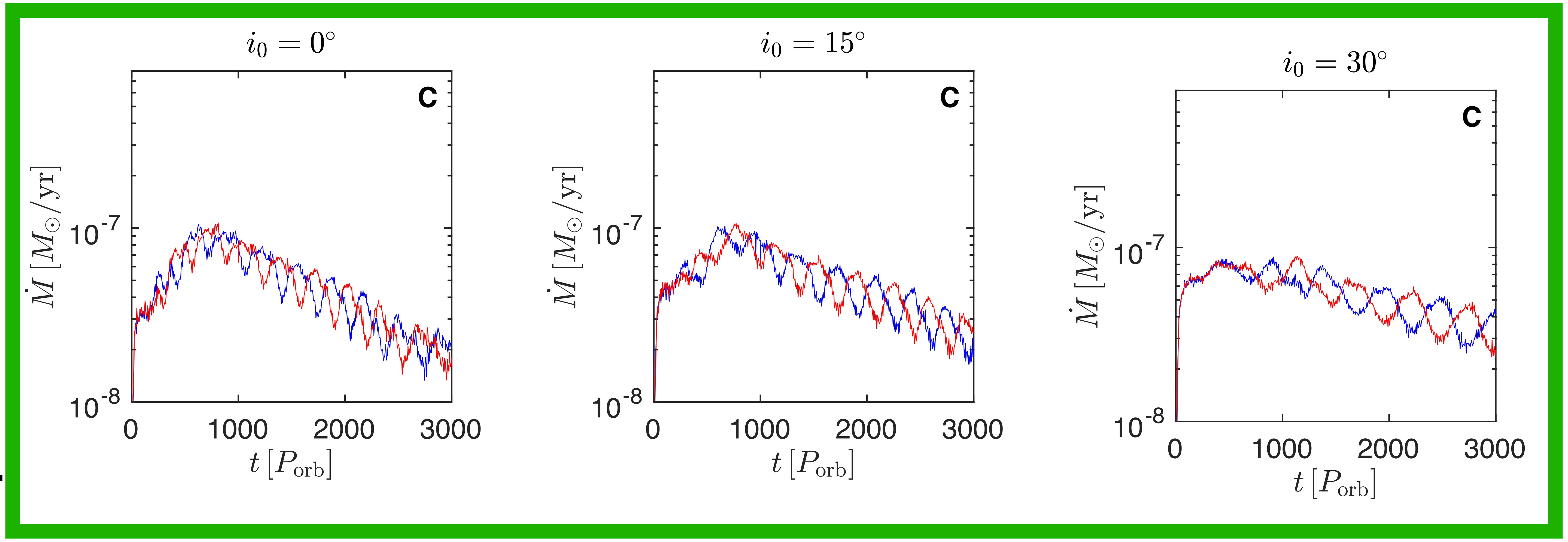


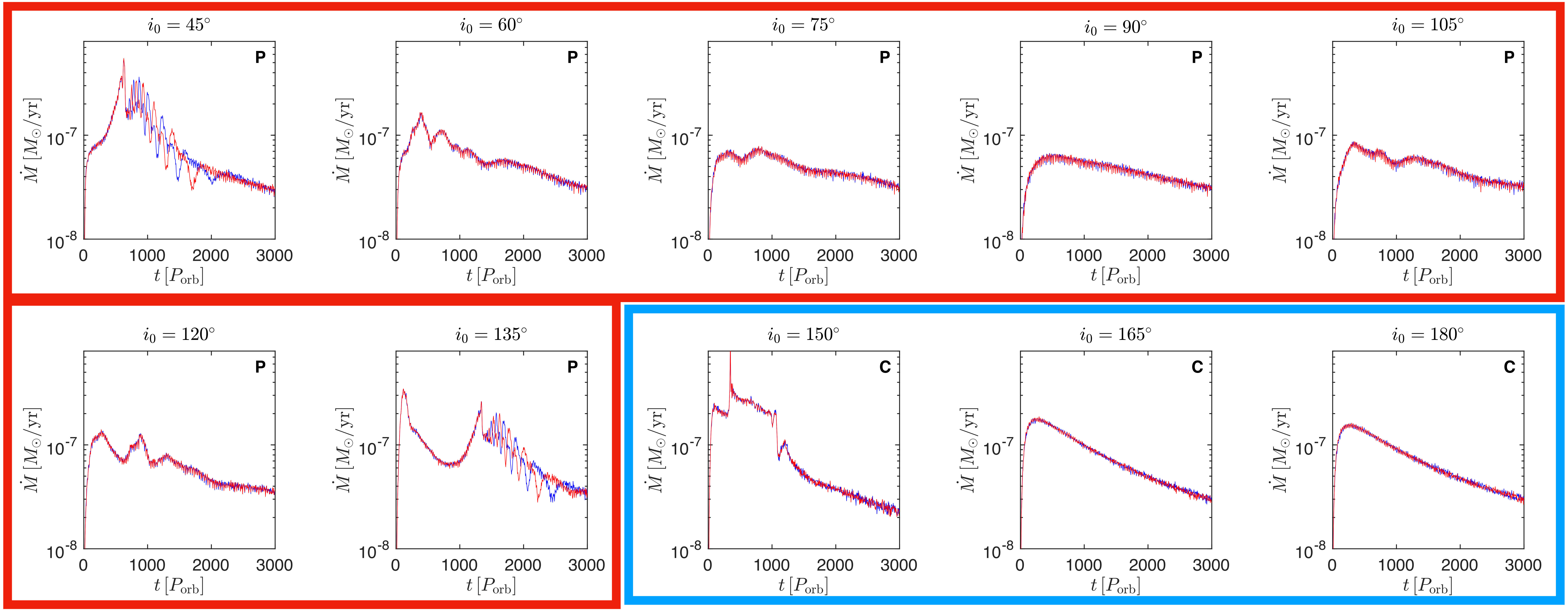

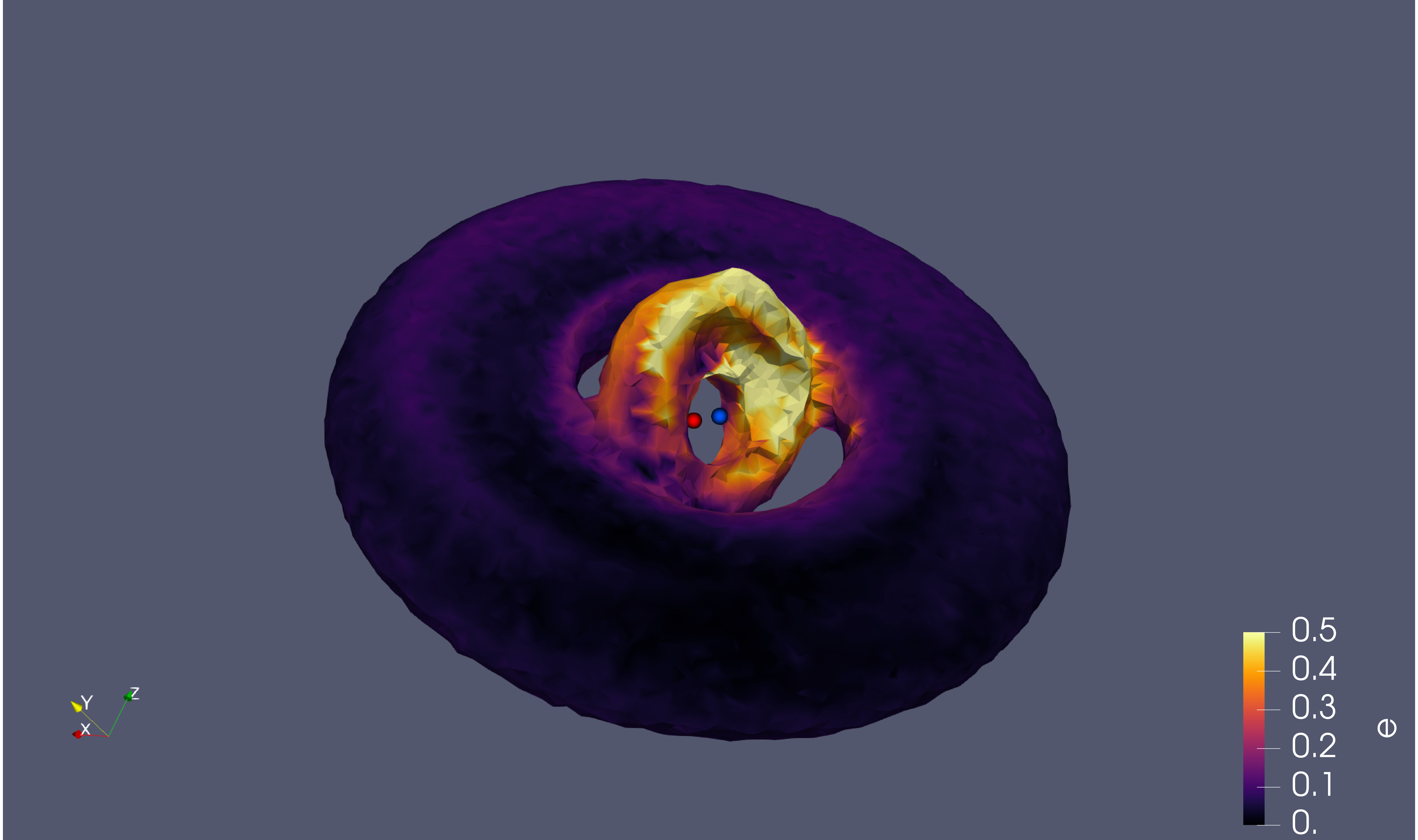

Y
Z
X
0.5
0.4
0.3
0.2
0.1
0.
e

# Gas-Dust Dynamics

- A useful measure for describing the coupling between dust and gas in the Epstein regime is the Stokes number, which is defined as:

$$\mathrm{St} = \frac{\pi}{2}\frac{\rho_{\mathrm{d}} s}{\Sigma_{\mathrm{g}}}$$

$\rho_{\mathrm{d}}$ : dust intrinsic density

$s$ : dust grain size

$\Sigma_{\mathrm{g}}$ : gas surface density

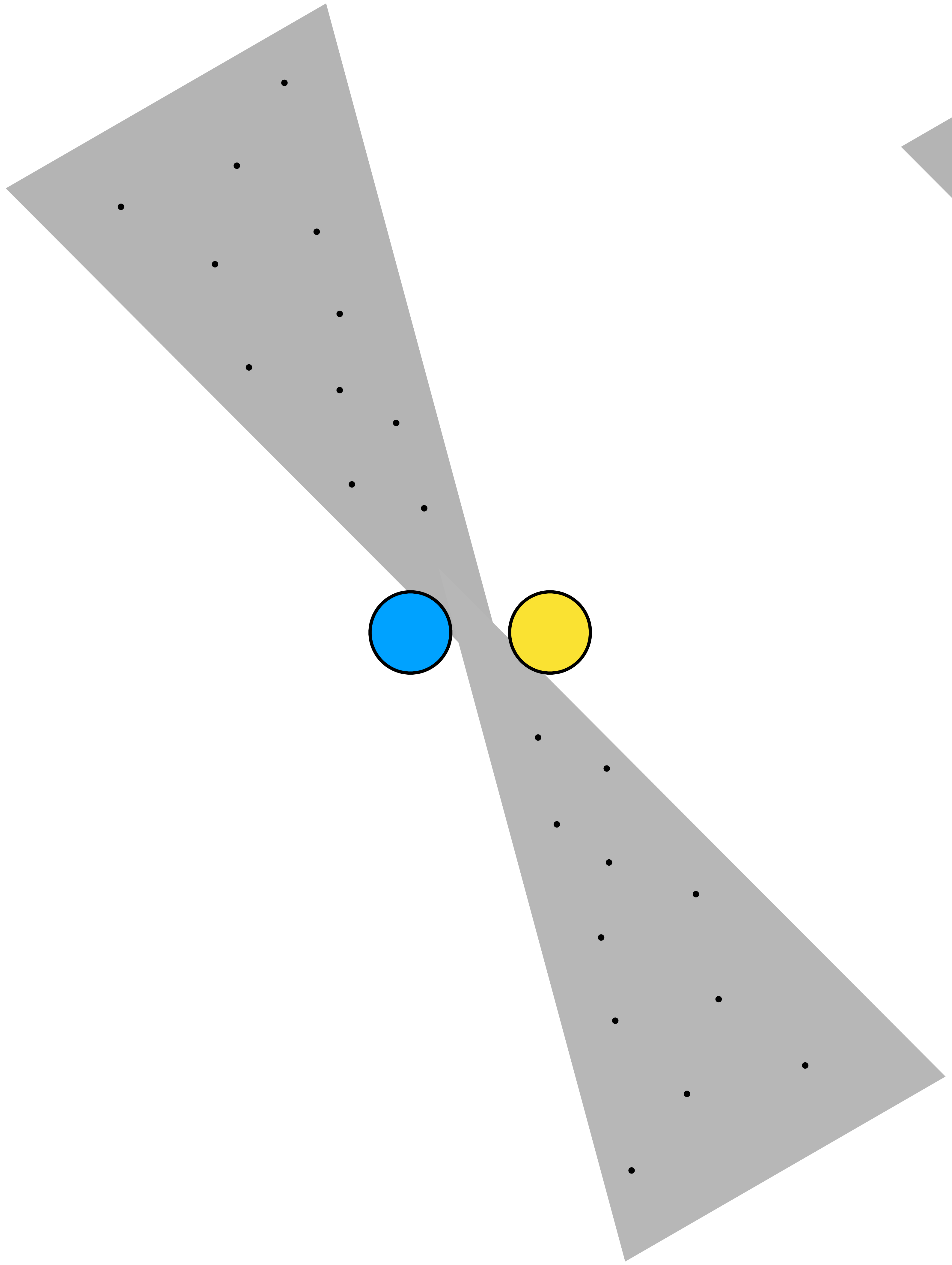

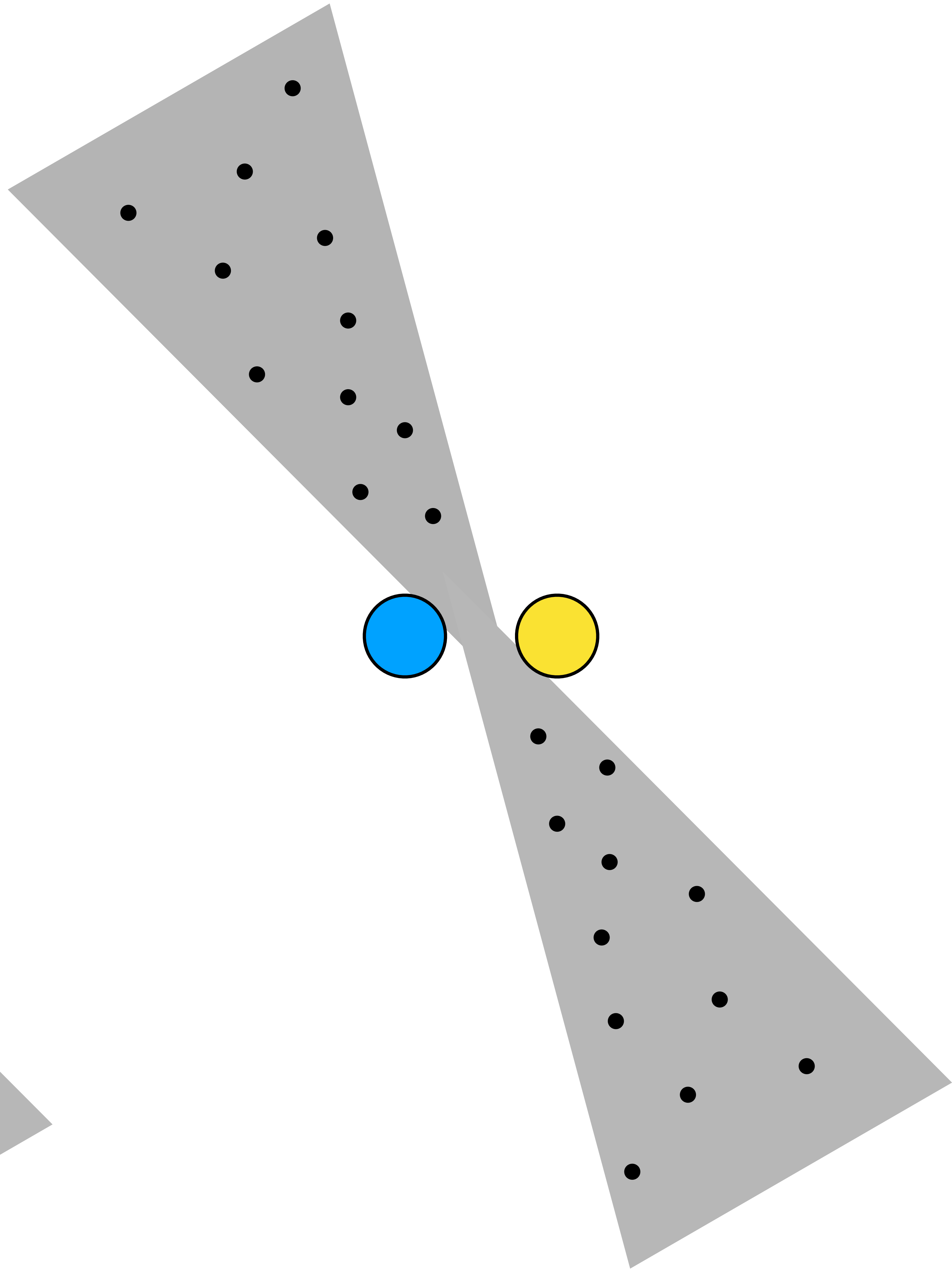

- Small grains $\mathrm{St} < 1$, are well coupled to the gas.
  - Precess at the same rate at the gas
- Large grains $\mathrm{St} \geq 1$, are weakly coupled to the gas.
  - Differential precession between gas and dust

# Misaligned Circumbinary Discs

- The differential precession between the gas and dust leads to the formation of dust traffic jams.
  - The velocity difference between the gas and dust components is zero, thus no radial drift could occur.

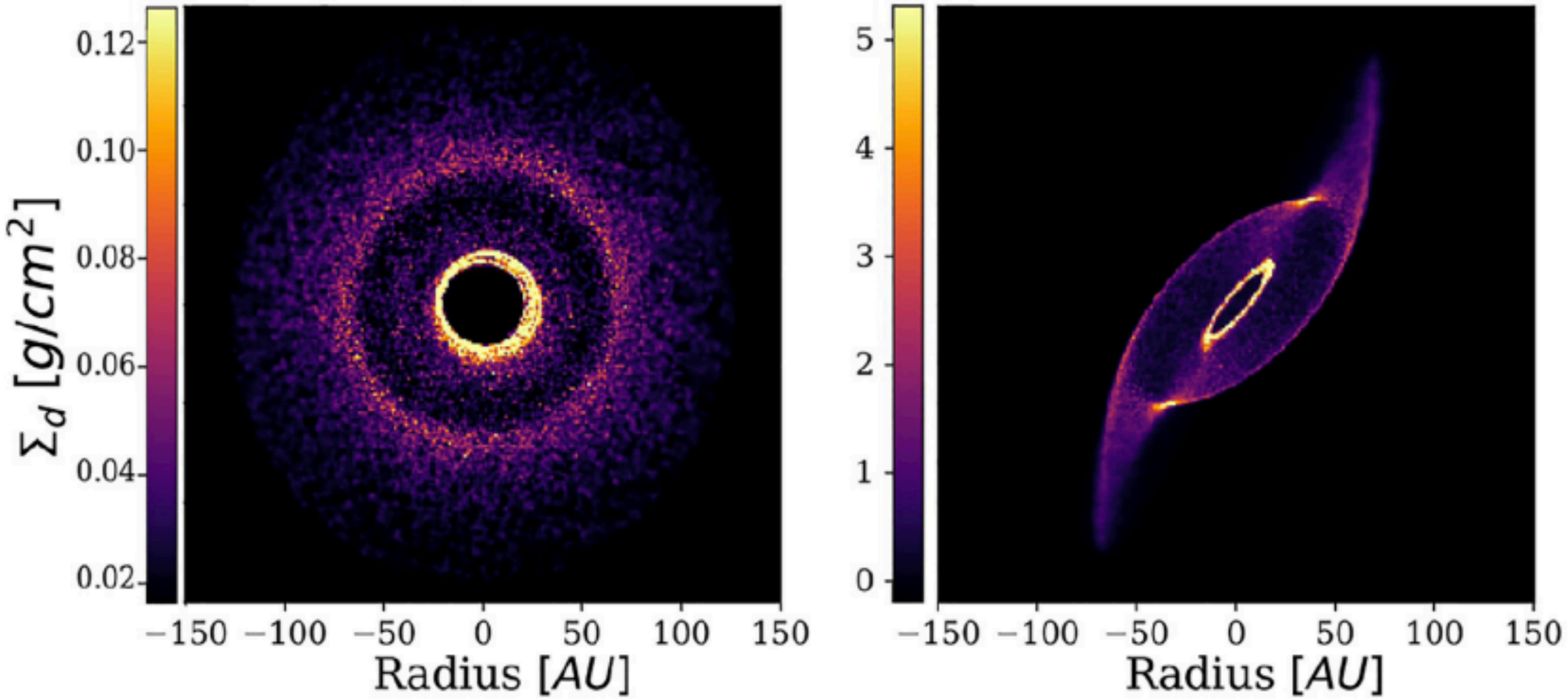


Aly et al. 2021

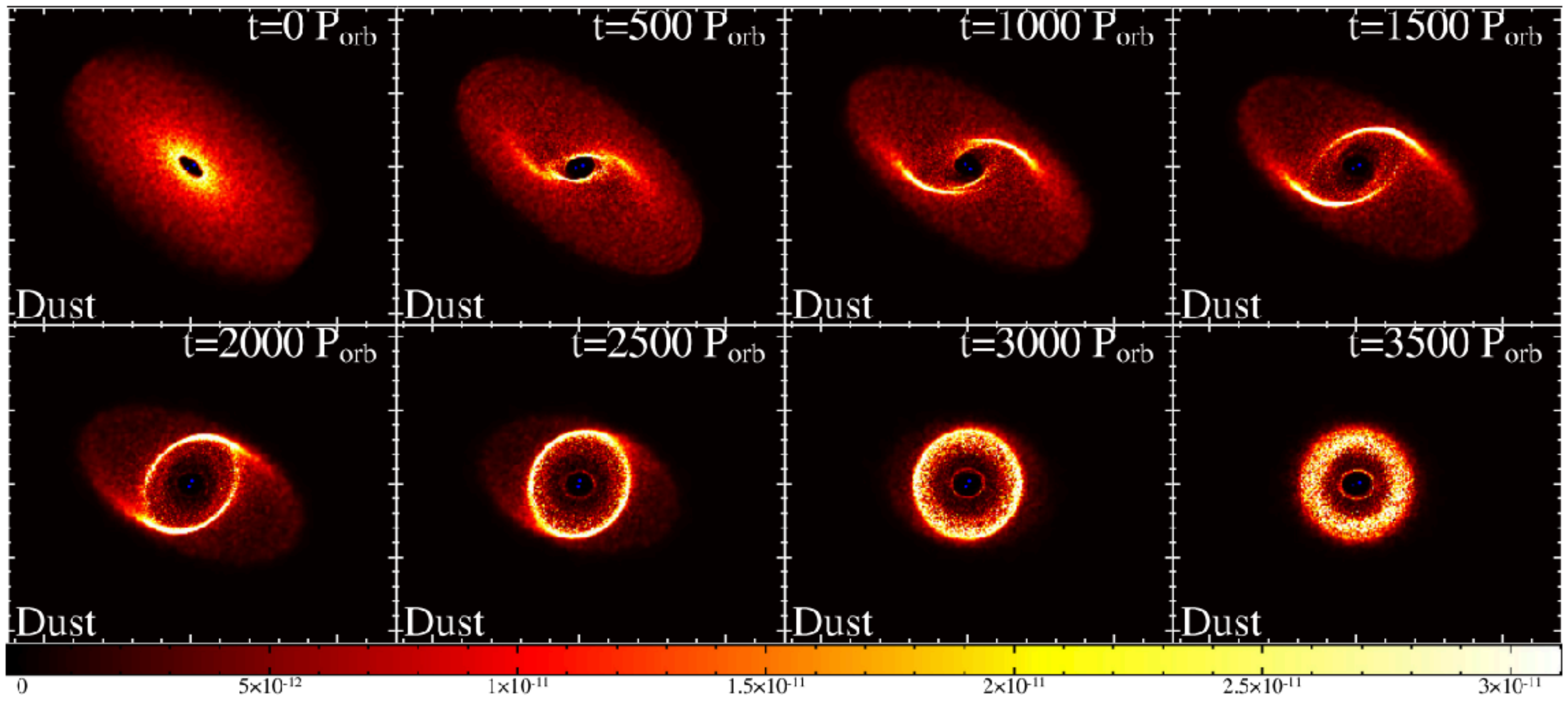


Longarini et al. 2021

# Formation of Dust Rings

- Differential precession between the gas and dust produce dust traffic jams.
- The dust traffic jams evolve into dense dust rings.
- This mechanism is robust — occurs whenever the disk is misaligned to the binary.
- Dust rings may be the sites for grain growth — planet formation

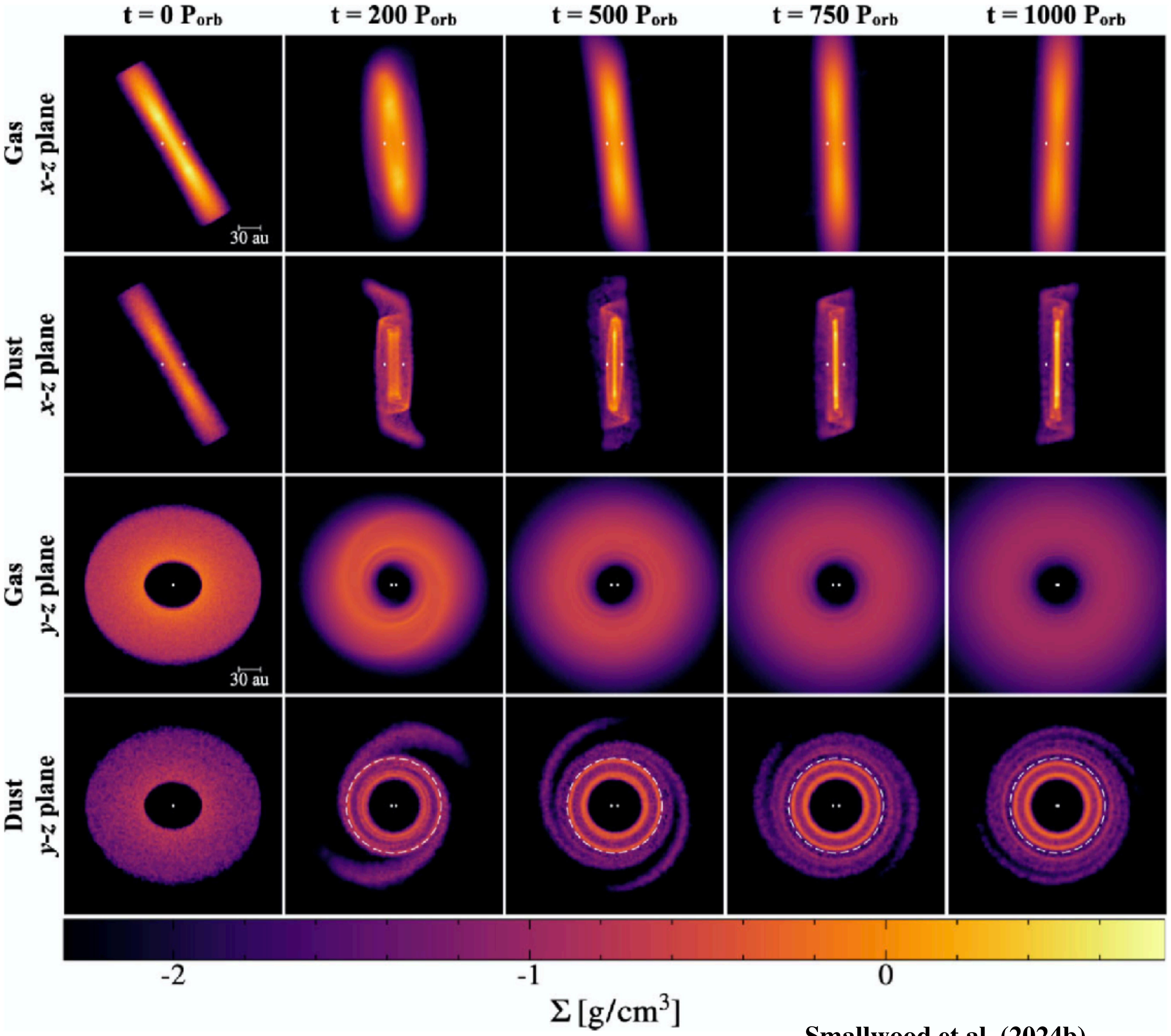


Smallwood et al. (2024b)

# Dusty Polar Circumbinary Disc

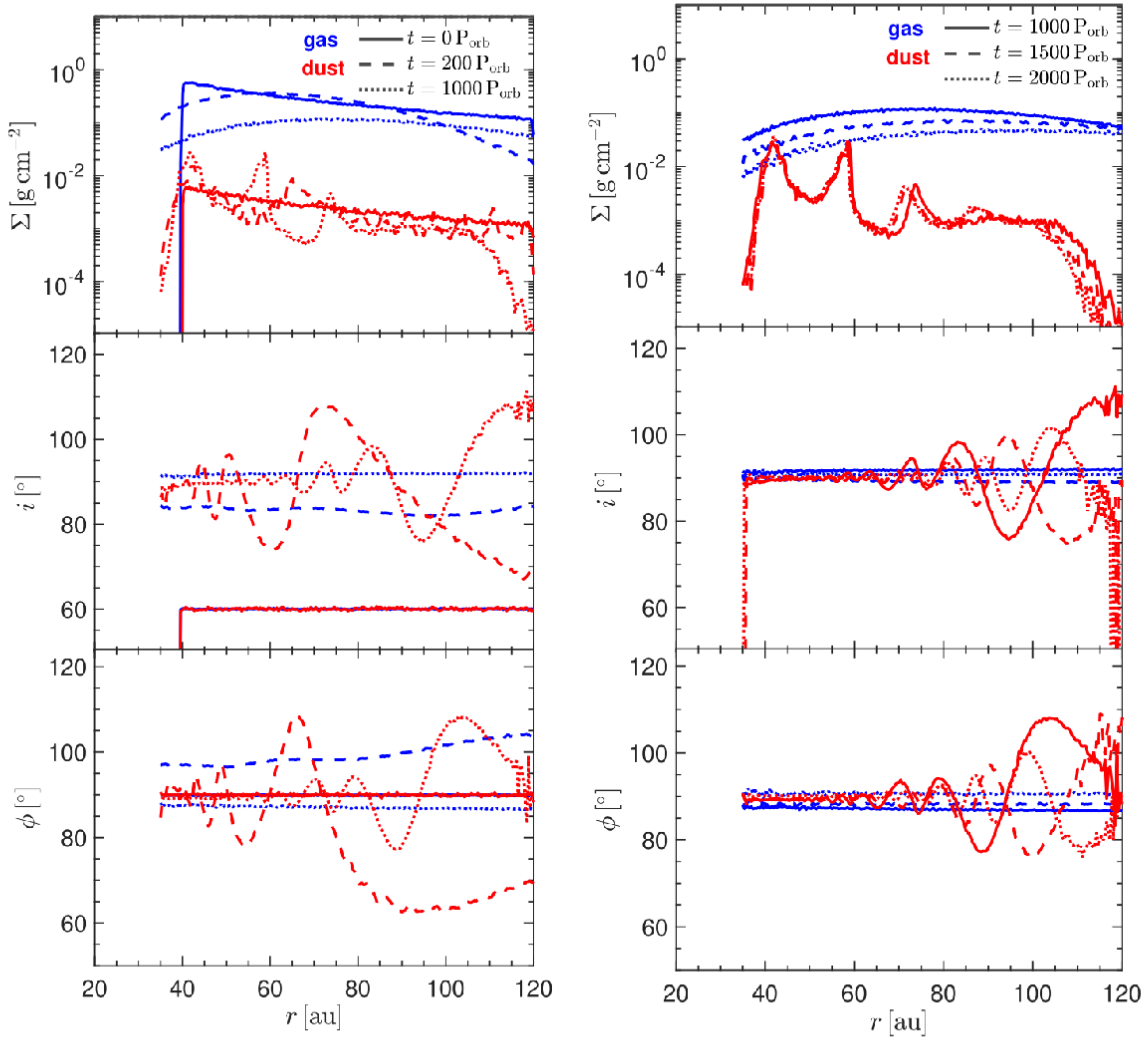


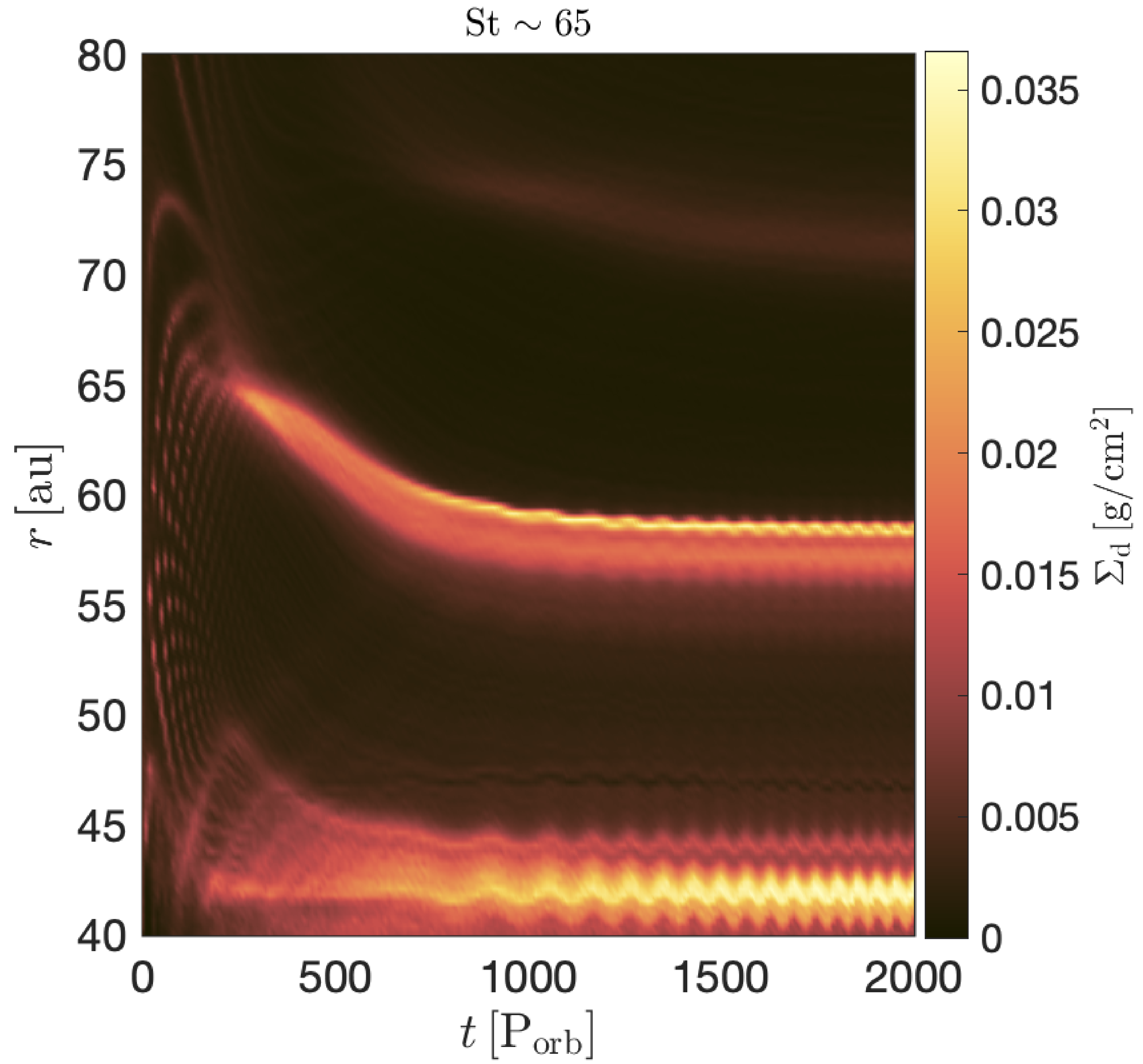


Smallwood et al. (2024b)

# Tracking Dust Particles

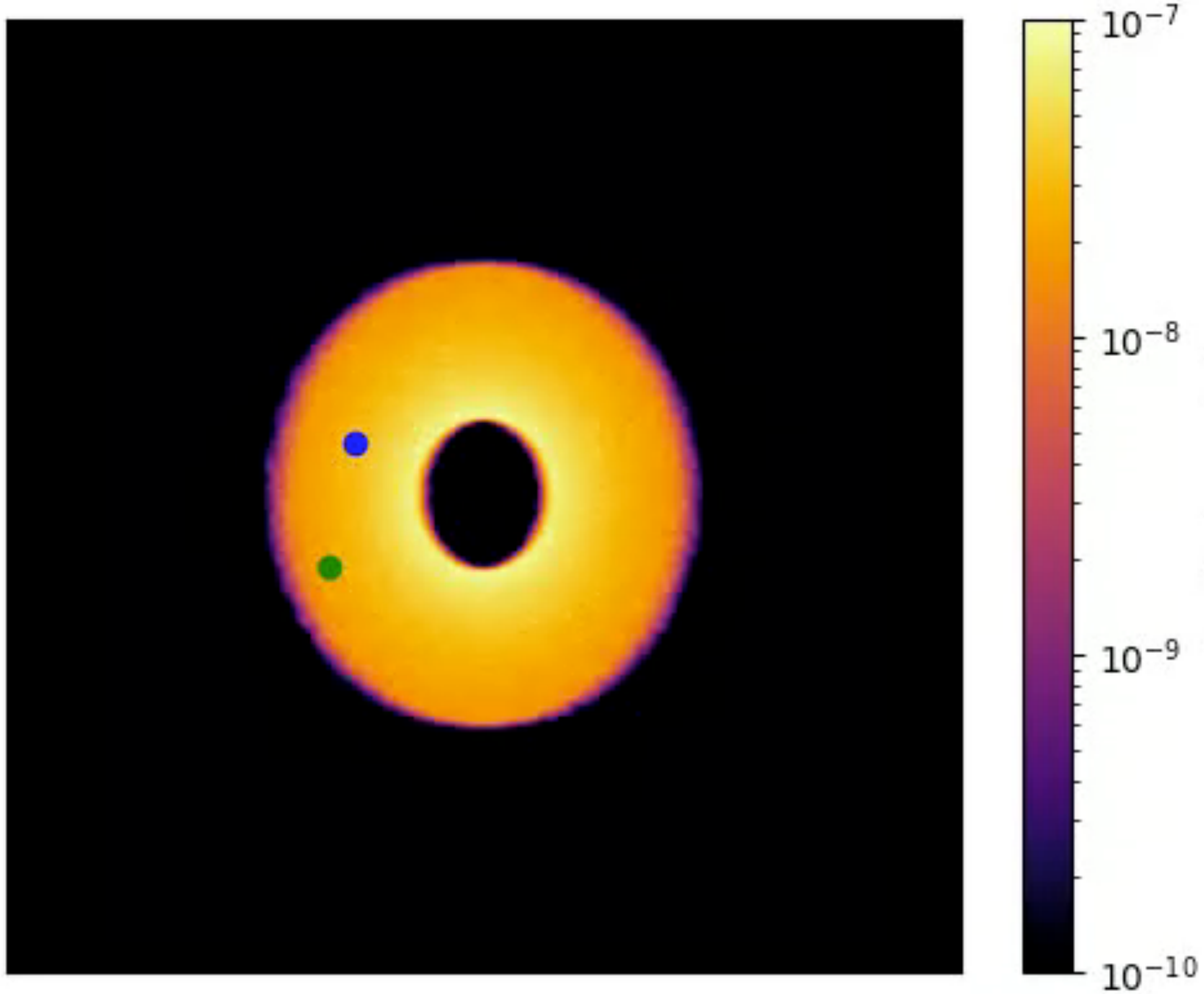


Analysed using SARRACEN (Harris & Tricco 2023)

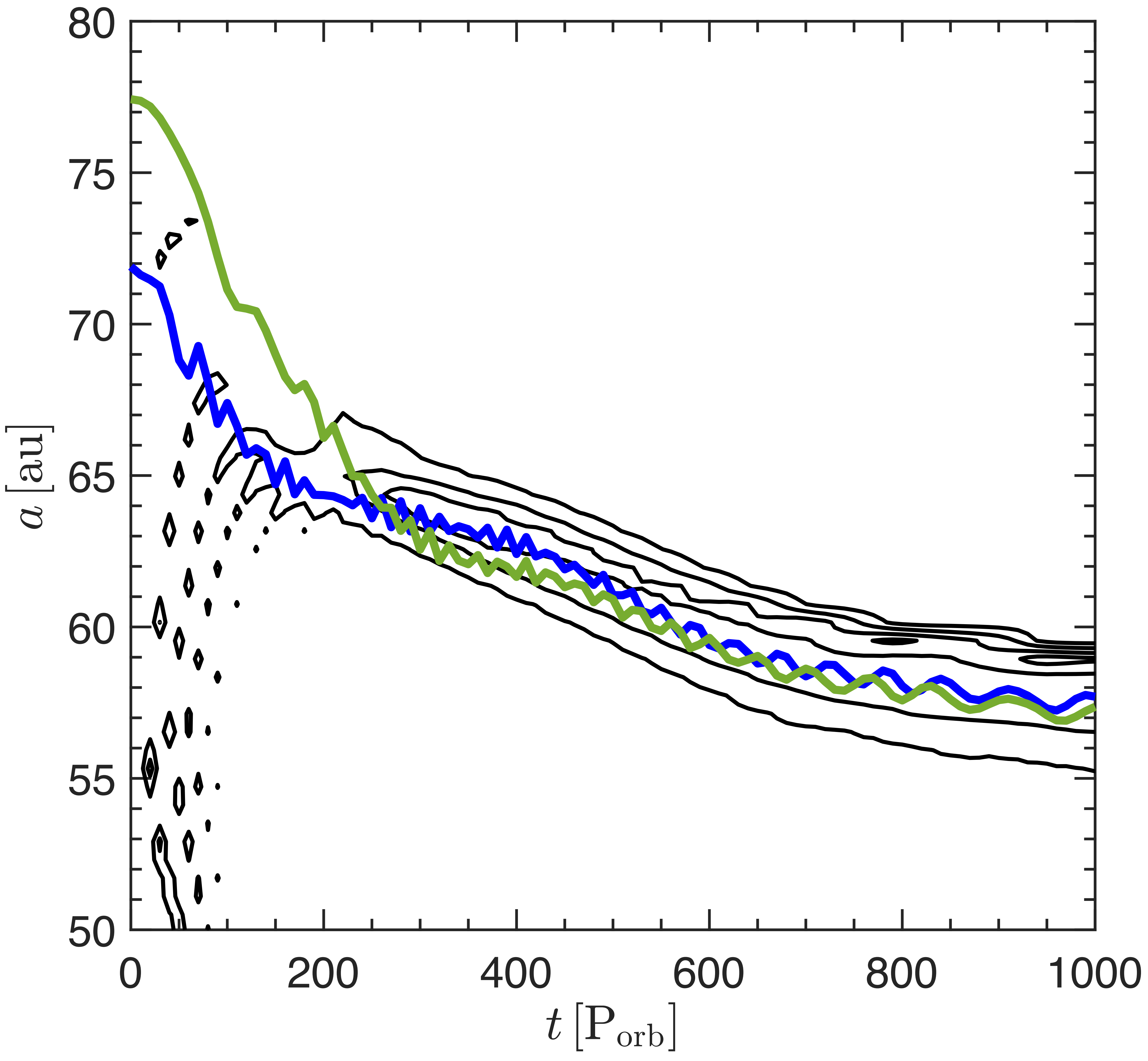


Smallwood et al. (2024b)

# Varying Grain Size

Smallwood et al. (2024b)

# Varying Disc Parameters

- Varying the disc parameters still leads to the formation of dust traffic jams.
  - Dust traffic jam formation is robust

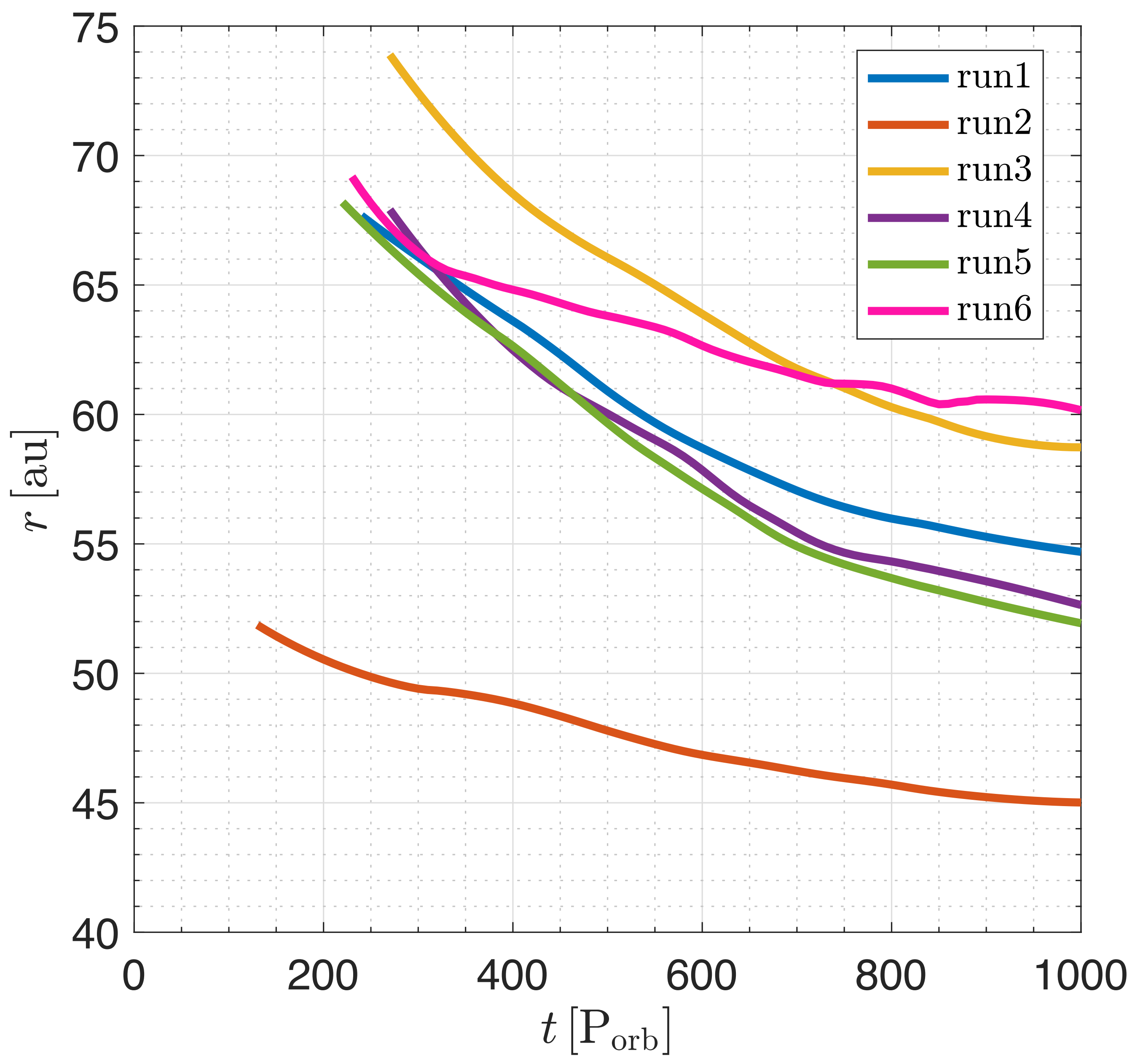


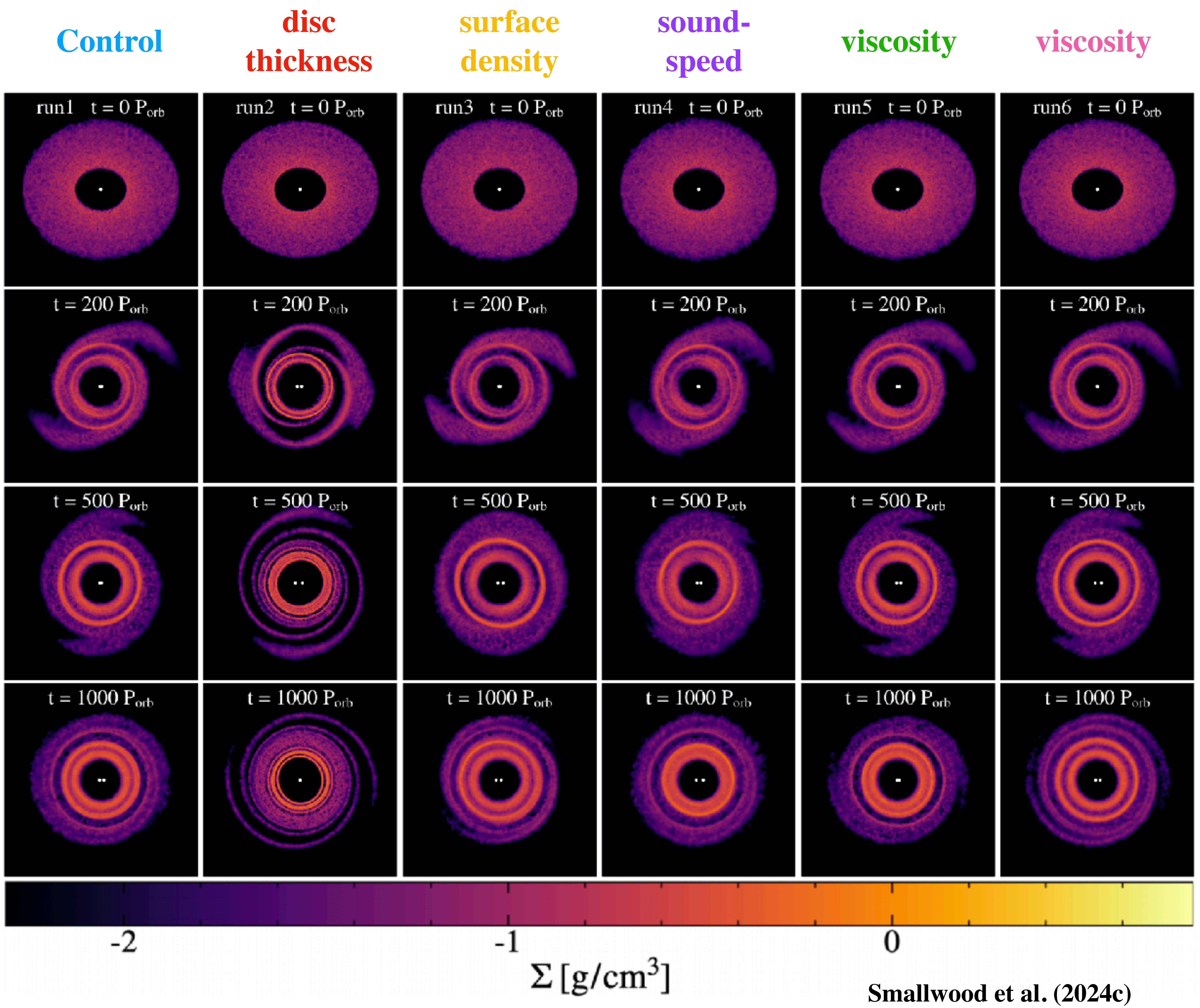


Smallwood et al. (2024c)

# Midplane dust-to-gas ratio

- The dust-to-gas ratio $\epsilon$ is heightened within the dust traffic jams.

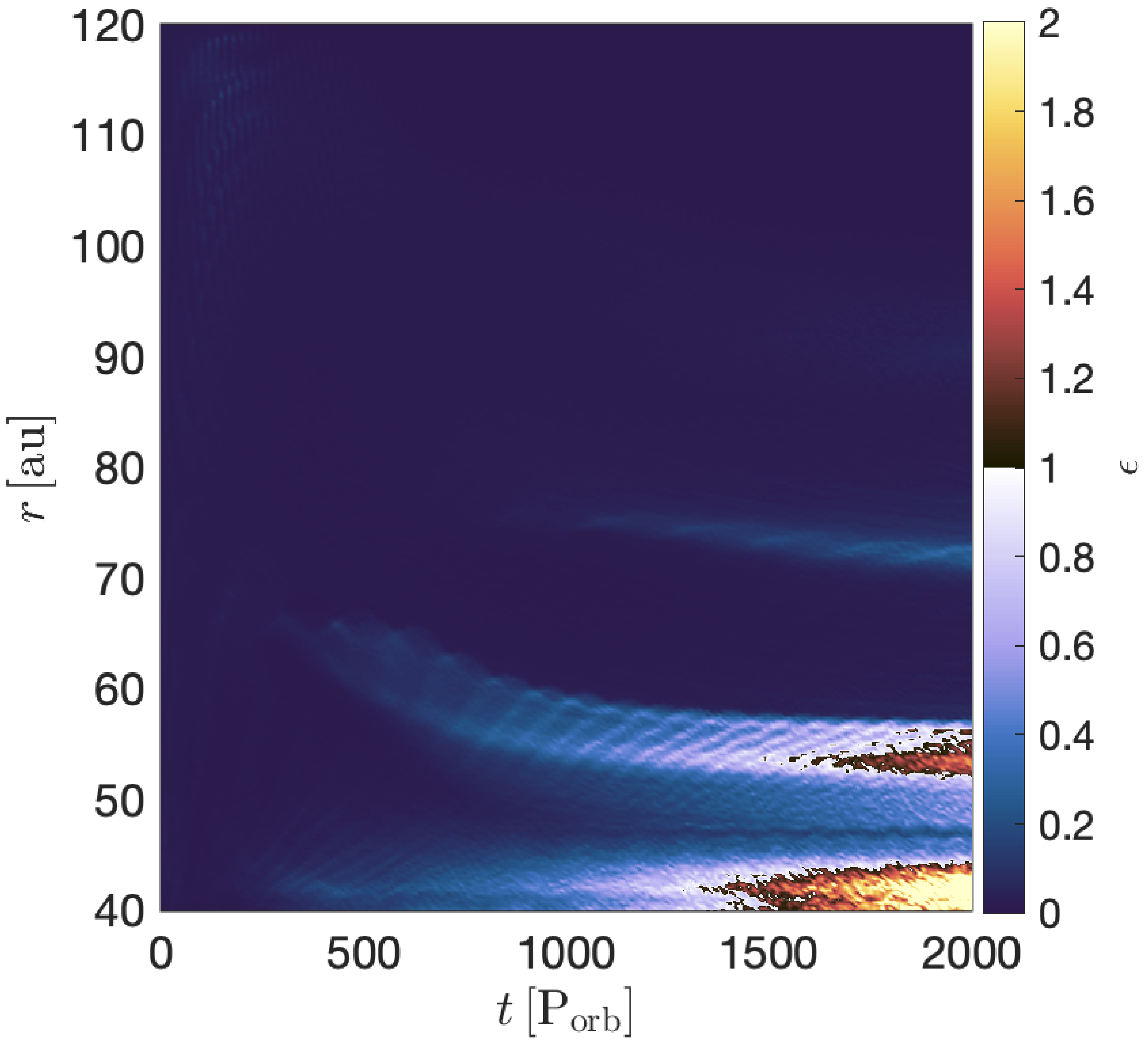


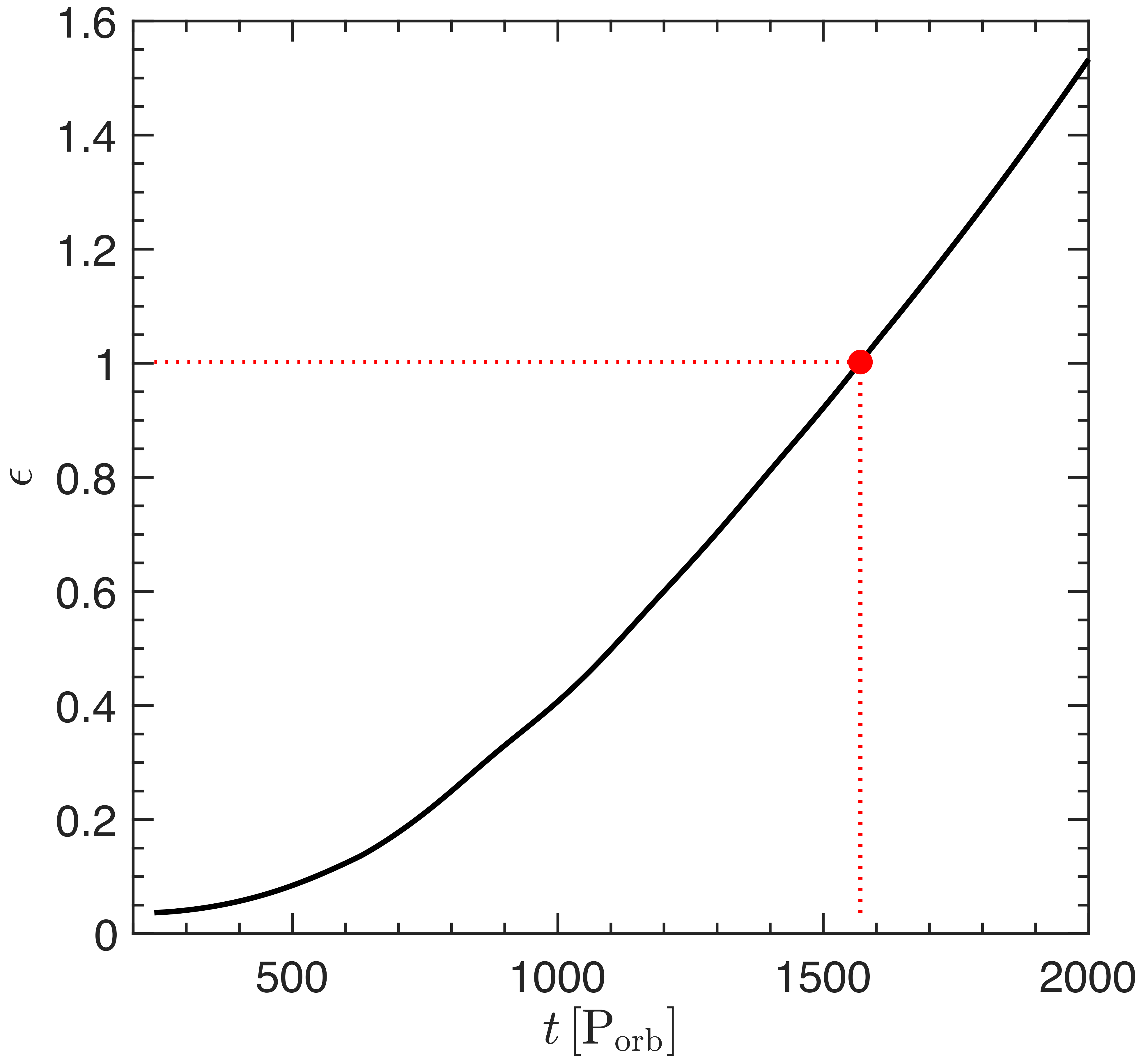


Smallwood et al. (2024c)

# Grain Growth via Streaming Instability

- **Streaming Instability** is a process where drag between solid particles and a gas disk causes particles to cluster and gravitationally collapse into planetesimals.

- Massive filaments form, reaching densities for gravitational collapse into asteroid-sized planetesimals, bypassing traditional formation barriers.

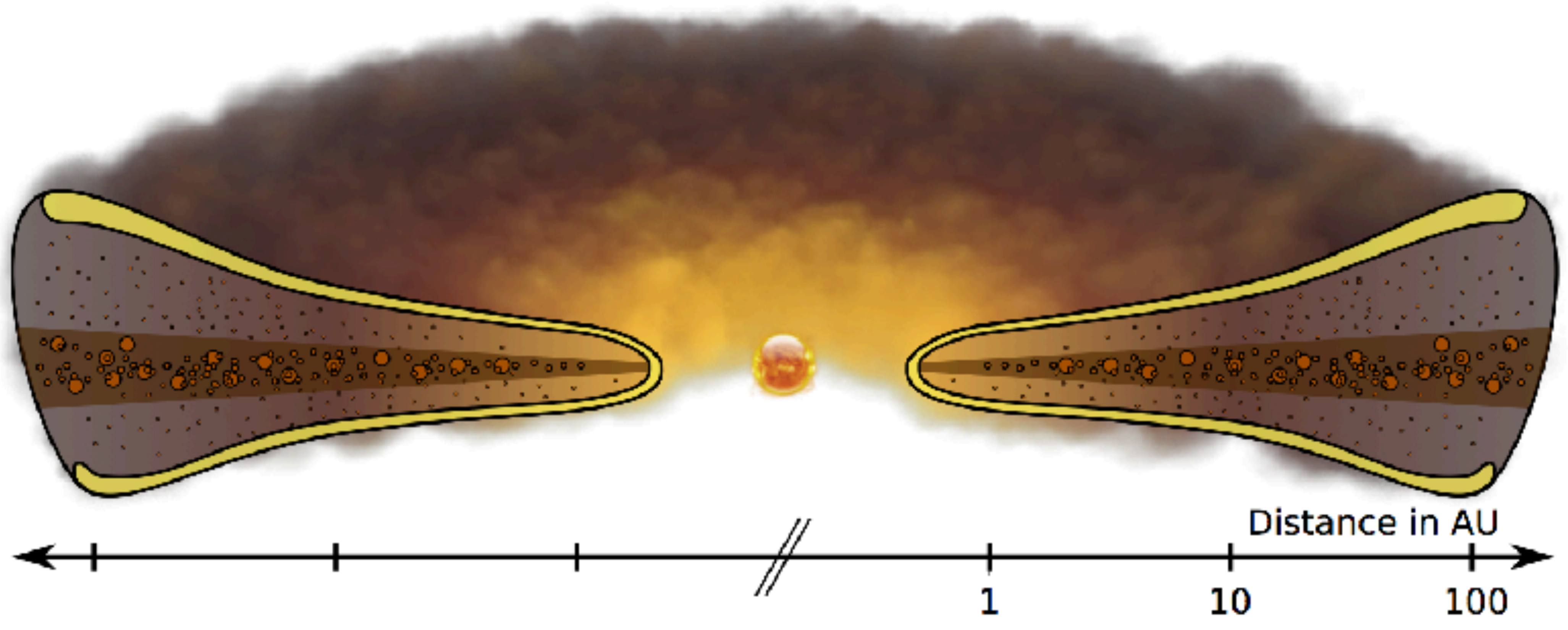


credit:

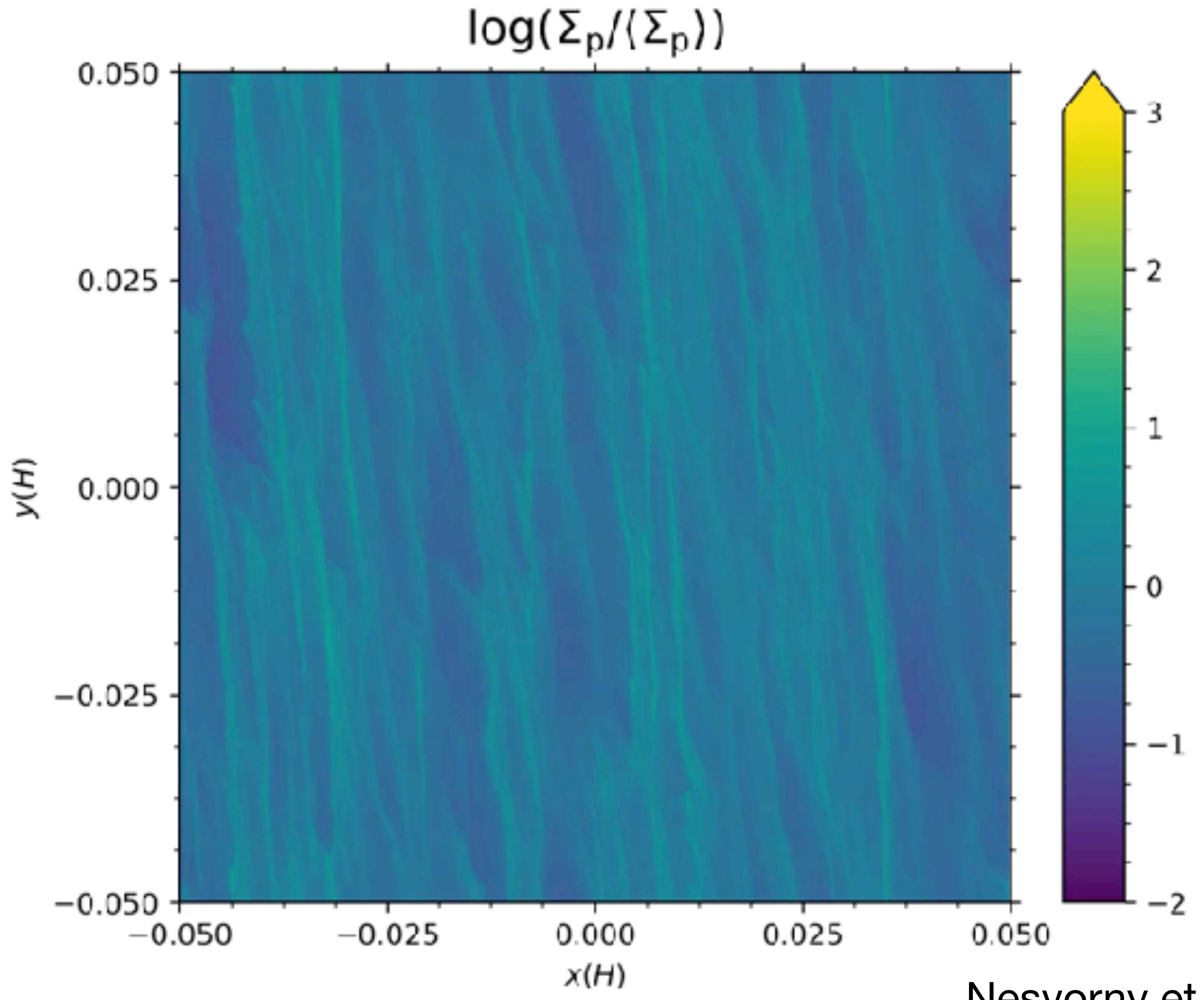


Nesvorny et al. 2019

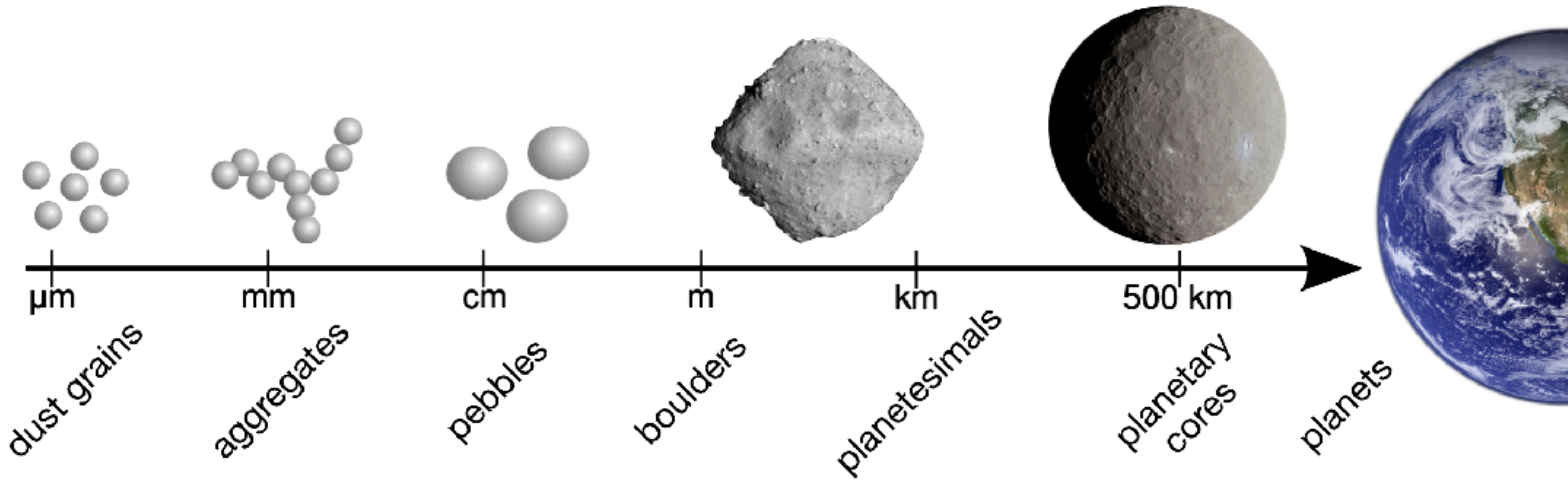

# Streaming Instability

- While current SPH simulations cannot resolve the SI, we can estimate SI growth rates given the midplane dust-to-gas ratios and particle sizes in our simulations.
  - —To this end, we numerically solve the linearized, two-fluid equations in the shearing box approximation (e.g. Chen & Lin 2020).

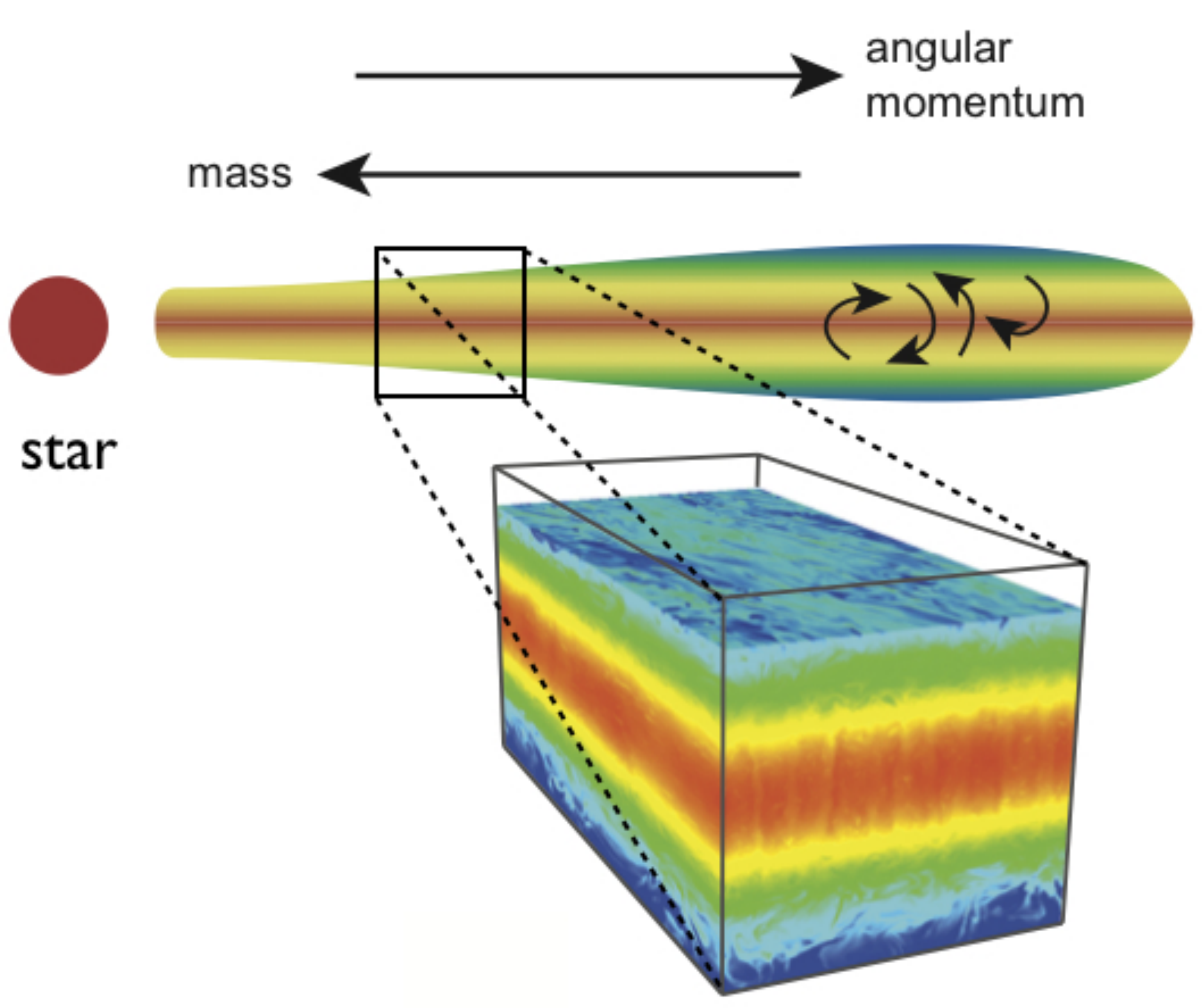


disk turbulence in local simulation

**credit: Jacob Simon**

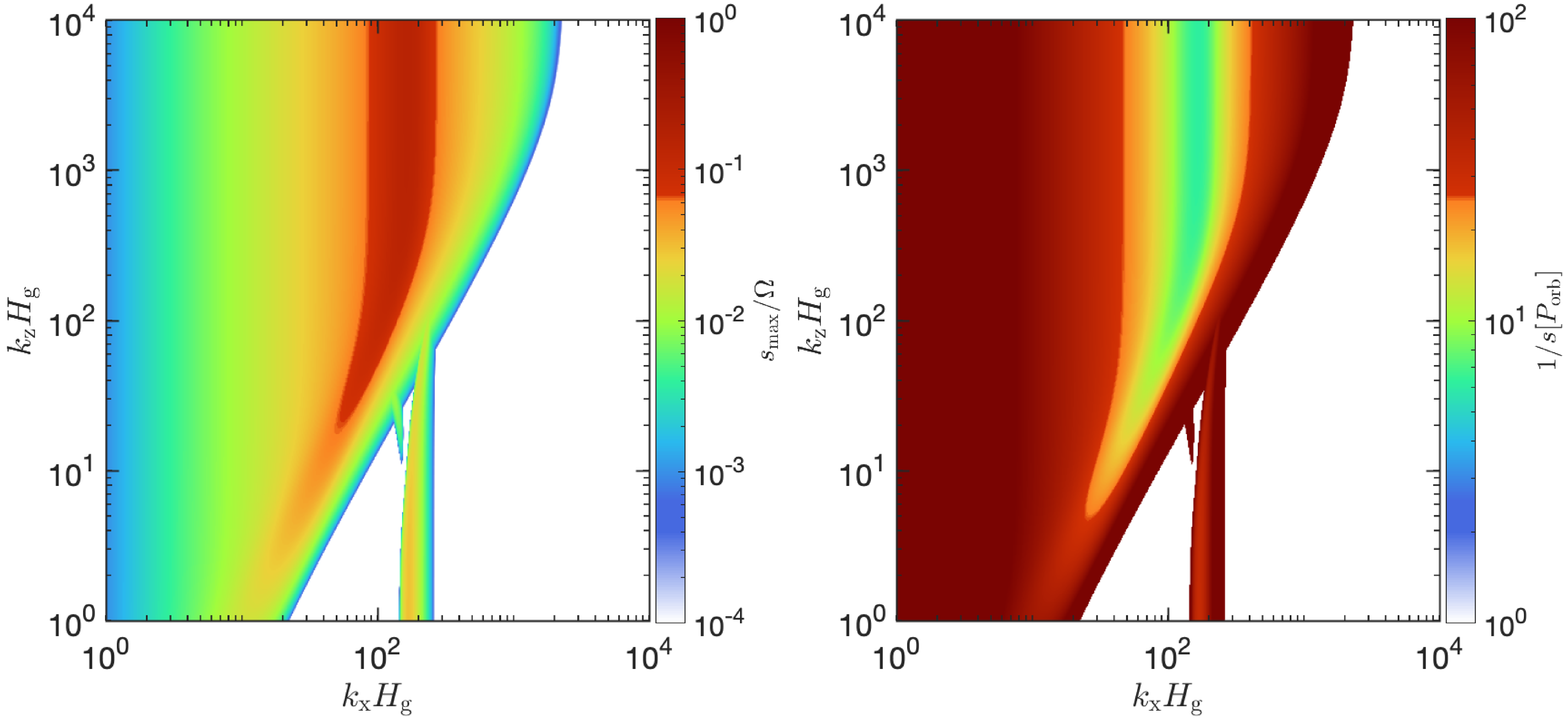


**Smallwood et al. (2024c)**

# Observational Signatures

- The next-generation Very Large Array (ngVLA) observations will be able to probe cm-sized dust grains.
- Operating within frequencies ranging from 1.2 GHz (25 cm) to 116 GHz (2.6 mm), the ngVLA will serve as a crucial bridge between ALMA and the forthcoming SKA.

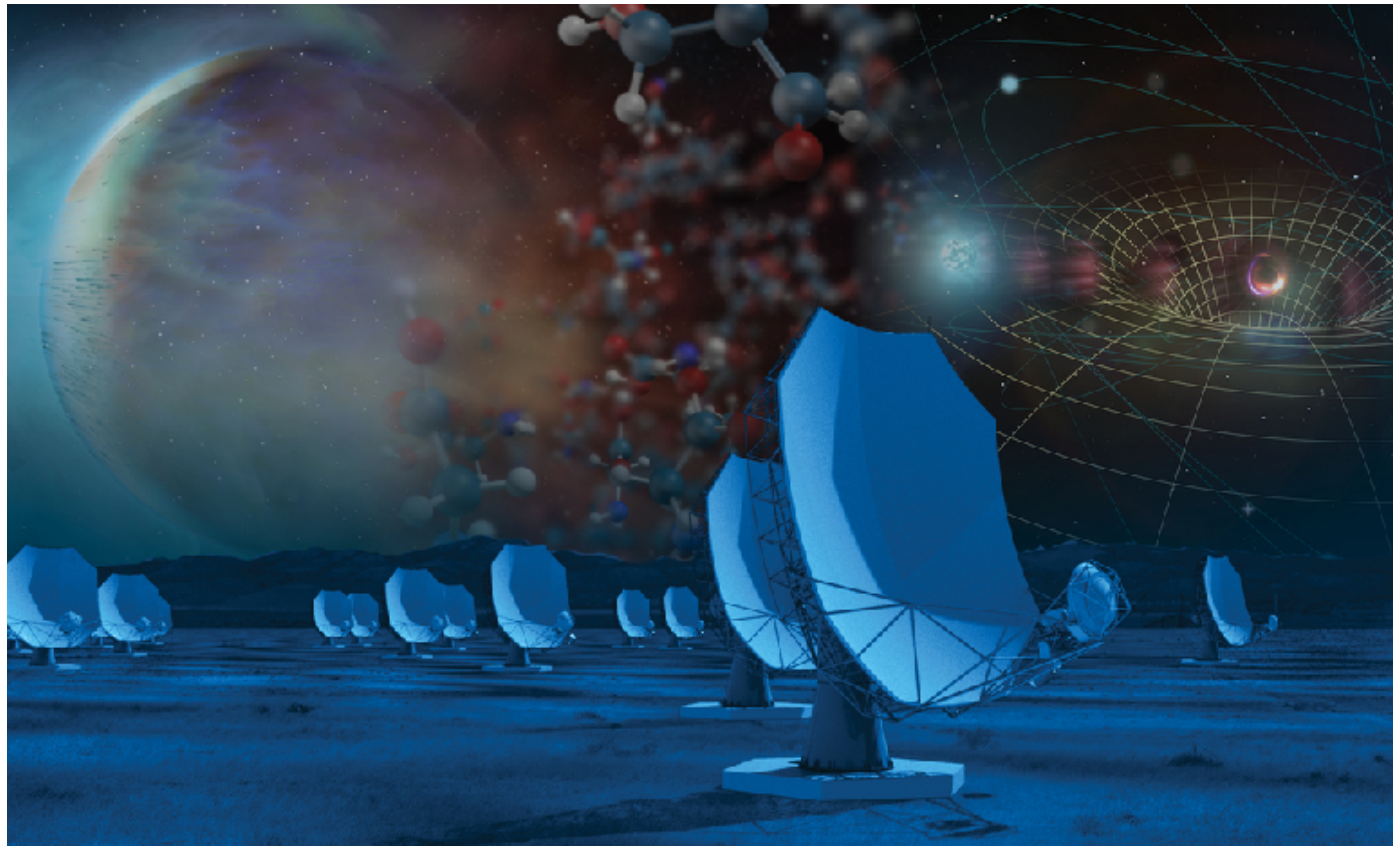

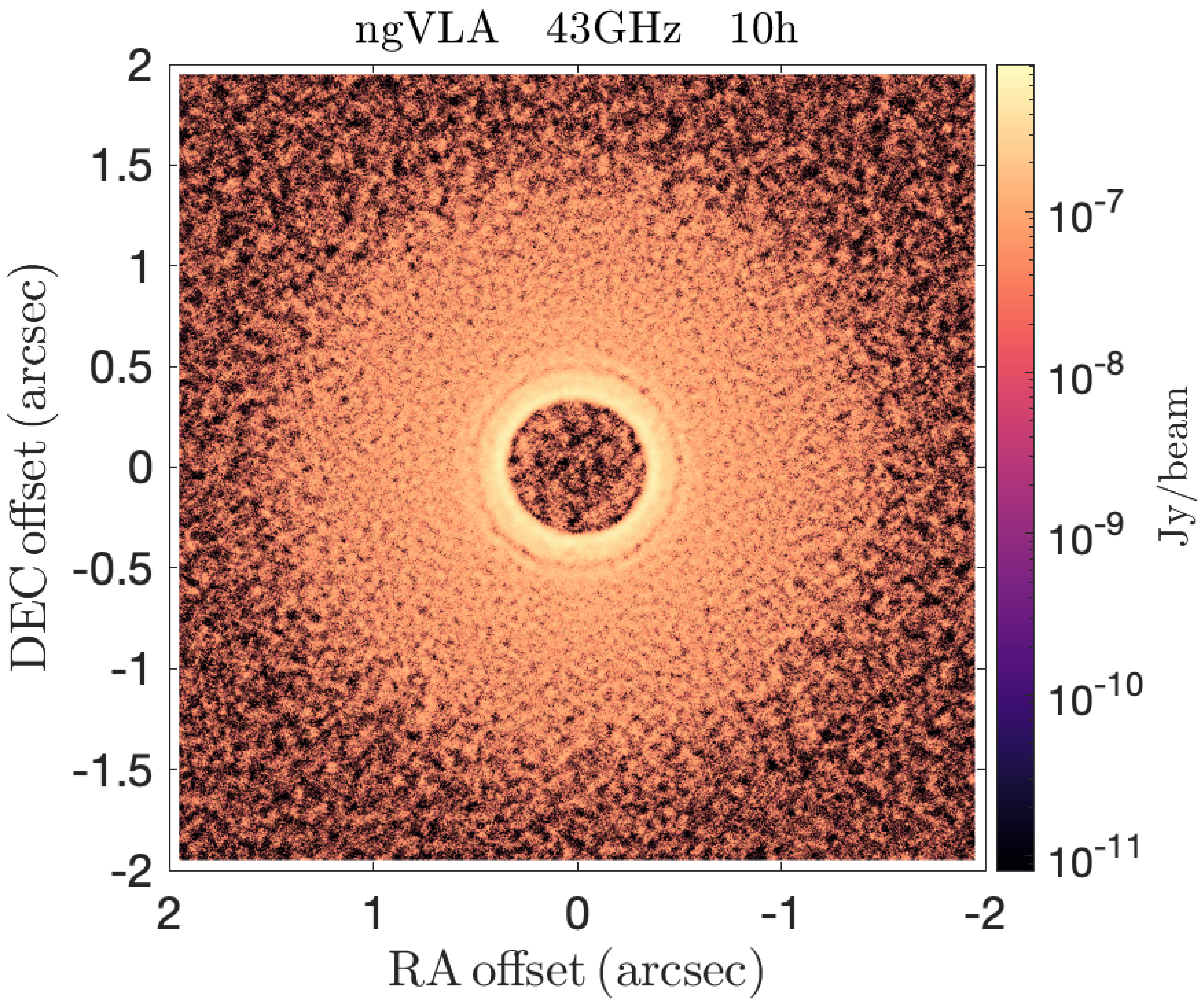


- The above ngVLA synthetic image shows the detection of dust traffic jams formed in misaligned circumbinary discs.

**Smallwood et al. 2024d**

# Polar Circumbinary Planets

- Polar circumbinary planets can be stable around eccentric binaries (Cuello & Giuppone 2019; Chen et al. 2020, Childs & Martin 2021).

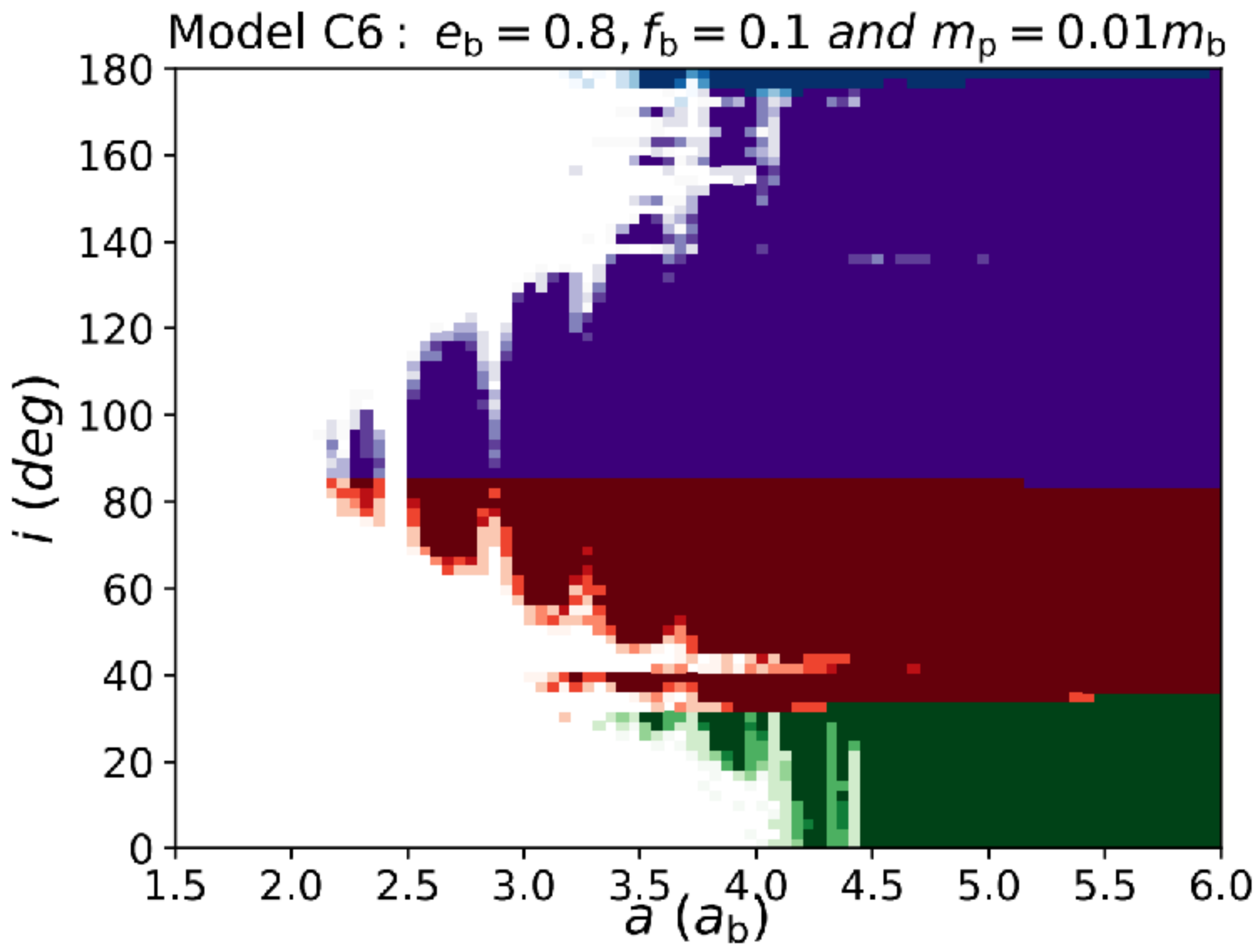


Chen et al. 2020

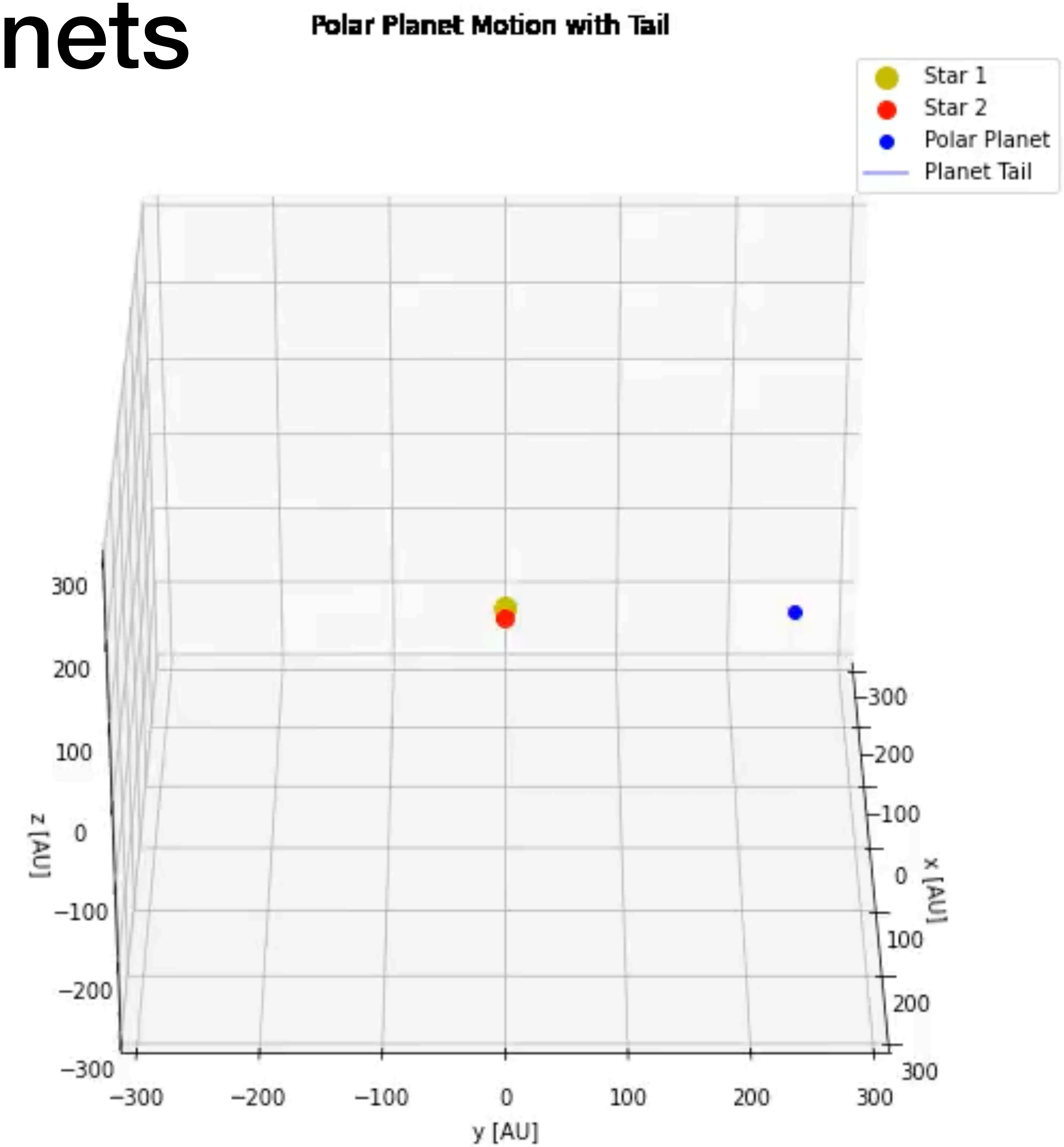

# Earth 2.0 Space Mission

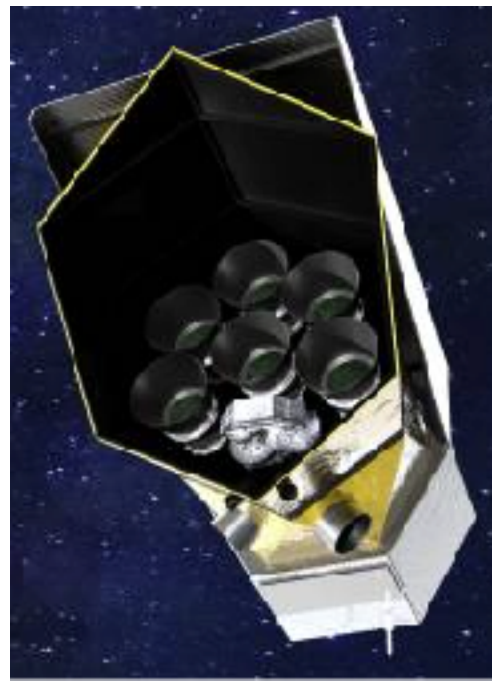

- ET will be expected to discover more than 100 circumbinary planets.
- <u>Key questions to address:</u>
    - What are the mass, size distribution, and orbital properties of circumbinary planets?
    - Are there some other populations of CBPs that are not detected in the current Kepler and TESS surveys: misaligned/polar ?

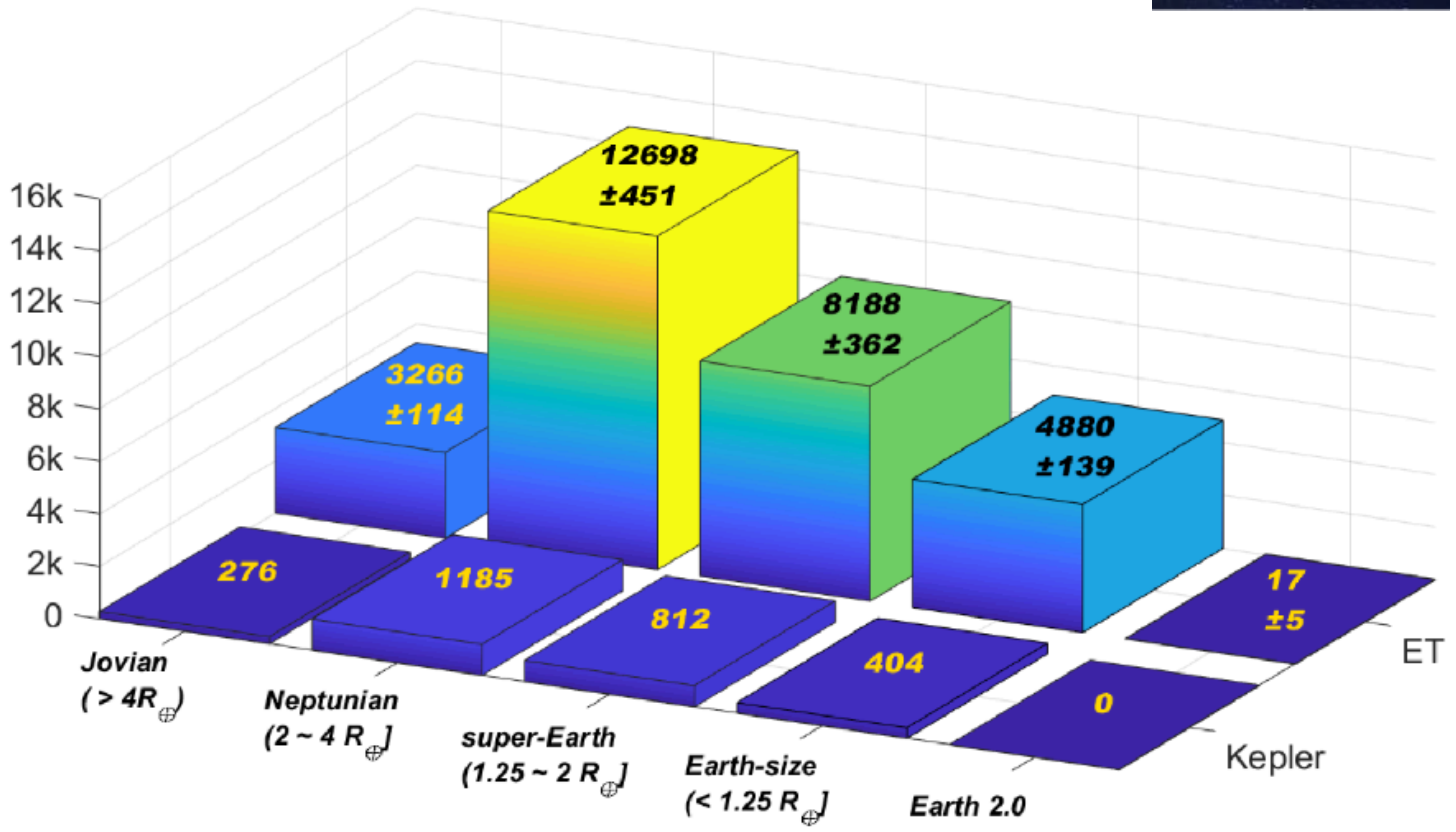


(Ge et al. 2022)

# Summary

- Circumbinary discs can align to a polar orbit with respect to the binary orbital plane.
- The differential nodal precession between the gas and dust during polar alignment produces dust traffic jams.
- Dust traffic jams with midplane dust-to-gas ratios exceeding unity, highlights the potential role of the streaming instability in fostering conditions conducive to the formation of polar planets.
- Dust traffic jams in initially misaligned circumbinary discs may be observable with the next generation telescopes, ngVLA.

# Pressure Gradient